AN ABSTRACT OF THE THESIS OF

Shannon A. McDowell for the degree of Master of Science in Chemical Engineering presented on September 14, 2012

Title: The Effects of Engineered Coatings and Natural Organic Matter on Nanoparticle Aggregation

Abstract approved:

Jeffrey A. Nason

In order to better predict the aggregation state of nanomaterials, the factors that influence aggregation must be understood. The combined effects of natural and engineered coatings have been shown to factor into nanoparticle aggregation behavior in preliminary research. In this study, aggregation behaviors of gold nanoparticles with two different engineered coatings were investigated in the presence of the monovalent electrolyte KCl and the divalent electrolyte $CaCl_2$. Aggregation studies were conducted using dynamic light scattering to determine the relative stability of the NMs in environments of varying ionic strength in the absence and presence of Suwannee River Natural Organic Matter (SRNOM). Coatings which provided primarily electrostatic stabilization were found to adhere closely to DLVO theory, while coatings which provided steric stability inhibited aggregation over a wide range of ionic strengths for both electrolytes. The presence of SRNOM was found to provide some electrostatic stability in the presence of KCl, but appeared to form agglomerates with calcium ions, especially at higher SRNOM concentrations.

©Copyright by Shannon A. McDowell
September 14, 2012
All Rights Reserved

The Effects of Engineered Coatings and Natural Organic Matter on Nanoparticle Aggregation

by
Shannon A. McDowell

A THESIS

submitted to

Oregon State University

in partial fulfillment of
the requirements for the
degree of

Master of Science

Presented September 14, 2012
Commencement June 2013

Master of Science thesis of Shannon A. McDowell presented on September 14, 2012.

APPROVED:

Major Professor, representing Chemical Engineering

Head of the School of Chemical, Biological, and Environmental Engineering

---

Dean of the Graduate School

I understand that my thesis will become part of the permanent collection of Oregon State University libraries. My signature below authorizes release of my thesis to any reader upon request.

Shannon A. McDowell, Author

ACKNOWLEDGEMENTS

The author would like to thank her advisor Dr. Jeffrey A. Nason for guidance and insight, Ty W. Callahan for major contributions to data collection, the National Science Foundation for creating this opportunity, and her friends and family for the support they have provided through this process.

TABLE OF CONTENTS

Page

Chapter 1: Introduction 1
1.1. Background and Motivation 1
1.2. Problem Statement 2
1.3. Significance 2
1.4. Objectives 3
1.5. Approach 3
Chapter 2: Literature Review 5
2.1. Physical Transformations 5
2.2. Electrostatic Forces 5
2.2.1. Introduction 5
2.2.2. DLVO Theory 6
2.3. Steric Forces 7
2.4. Natural Organic Matter 8
2.5. Engineered NM Coatings 10
Chapter 3: Materials and Methods 12
3.1. Nanoparticles 12
3.2. Suwannee River Natural Organic Matter 13
3.3. Electrolyte Solutions 14
3.4. NP-NP Aggregation Measurements 14
3.5. Zeta Potential Measurements 17
Chapter 4: Results and Discussion 18
4.1. Citrate-AuNPs 18
4.2. Carboxyl-AuNPs 23
Chapter 5: Conclusions 34
5.1. Key Findings 34
5.2. Implications 35
5.3. Further Research 36
References 39
APPENDIX 45

LIST OF FIGURES

Figure Page

Figure 1. Molecular structures of the capping agents used to stabilize gold nanoparticles, including an electrostatically-bound citrate miltilayer (citrate-AuNP) and covalently-bound PEG chains with a carboxyl end-group (carboxyl-AuNP) 13

Figure 2. Aggregation of 1 mg/L citrate-AuNPs exposed to increasing concentrations of KCl. Initial aggregation rate was calculated as shown for citrate-AuNP exposure to 100 mM KCl. 16

Figure 3. Determination of the CCC for 1 mg/L citrate-AuNPs in KCl is calculated using attachment efficiencies as a function of electrolyte concentration. 16

Figure 4. Aggregation of 1 mg/L citrate-AuNPs as a function of time in the presence of 1 mg C/L as SRNOM and increasing concentrations of KCl..... 19

Figure 5. Attachment efficiencies of citrate-AuNPs as a function of KCl concentration in the presence of 0 mg C/L as SRNOM and 1 mg C/L as SRNOM. 19

Figure 6. Aggregation of 1 mg/L citrate-AuNPs as a function of time for increasing $CaCl_2$ concentration. (A) in the presence of $CaCl_2$; (B) in the presence of 1 mg C/L as SRNOM and $CaCl_2$. 21

Figure 7. Attachment efficiencies for citrate-AuNPs in the presence of 0 mg C/L as SRNOM and 1 mg C/L as SRNOM. CCC concentrations, in mM $CaCl_2$, are shown in the inset. 22

Figure 8. Visual depiction of a Ca^{2+} ion bridging between two negatively-charged NOM species, which in turn are adsorbed to the surfaces of two particles... 23

Figure 9. Particle size as a function of time for carboxyl-AuNPs exposed to increasing KCl concentrations. (A) carboxyl-AuNPs with 0 mg C/L as SRNOM. Noise in the 0 mM KCl sample, due to dust, was removed when it exceeded 3 standard deviations of the average size. (B) carboxy-AuNPs with 1 mg C/L SRNOM. 24

Figure 10. Particle size over time for 1 mg/L carboxyl-AuNPs in several concentrations of $CaCl_2$. 25

Figure 11. Aggregation behavior of 1 mg/L carboxyl-AuNPs exposed to 1mg C/L as SRNOM and varying concentrations of $CaCl_2$, as noted in the inset. 27

Figure 12. Change in hydrodynamic diameter, D_h, over time for carboxyl-AuNPs in several concentrations of SRNOM (reported as mg C/L) and 150 mM $CaCl_2$. 29

Figure 13. Hydrodynamic diameter of 1 mg/L carboxyl-AuNPs in solutions of several SRNOM concentrations, reported as mg C/L. D_h is reported after 30 min of exposure to $CaCl_2$, as a function of $CaCl_2$ concentration. 29

Figure 14. Change in hydrodynamic diameter, D_h, over time for carboxyl-AuNPs in a solution of 10 mg C/L as SRNOM. No electrolyte was present in solution. 30

Figure 15. SRNOM size over time in 250 mM $CaCl_2$. 31

Figure 16. Comparison between TR-DLS runs with and without the presence of carboxyl-AuNPs in a solution of 150 mM $CaCl_2$. (A) compares between trials at 5 mg C/L as SRNOM and (B) compares between trials at 10 mg C/L as SRNOM. 32

LIST OF APPENDIX FIGURES

Figure Page

Figure 1. Aggregation of citrate-stabilized AuNPs in KCl. (a) TR-DLS profiles of Dh for 1 mg/L citrate-stabilized AuNPs in KCl solutions of varying ionic strength. (b) Attachment efficiencies for citrate-stabilized AuNPs as a function of KCl concentration. The CCC calculated from Figure 1b is 56 mM KCl.……49

Figure 2. Aggregation of cit-AuNPs in the presence of NOM isolates and KCl. (a-d) TR-DLS profiles of cit-AuNPs in 1 mg C/L as SRFA, SRHA, SRNOM and PLFA, respectively……51

Figure 3. Attachment efficiencies of AuNPs in the presence of 1 mg C/L of the four NOM isolates. CCC concentrations for AuNPs in each NOM isolate are shown in the inset table……...……53

Figure 4. The influence of NOM concentration of cit-AuNP colloidal stability. Attachment efficiencies as a function of DOC for 1 mg/L cit-AuNPs in 80 mM KCl and varying concentrations (0-10 mg C/L) of each of the four NOM isolates…….....…..55

The Effects of Engineered Coatings and Natural Organic Matter on Nanoparticle Aggregation

Chapter 1: Introduction

1.1.Background and Motivation

Engineered nanomaterials (ENMs) are integral to current technological and scientific advancements. A broad spectrum of products utilize ENMs, including micro-electronics, solar energy capture systems, and advanced medical treatment techniques. It is estimated that over one thousand consumer products contain NMs (also referred to as nanoparticles, NPs), and this figure is predicted to increase with time [1]. Nanomaterials are defined as having at least one dimension less than 100 nm. Because of their small size, NMs have a relatively large surface area to volume ratio. With so much area available for reactions, NMs often exhibit unique properties and reactivity compared with similar materials of a larger size [2, 3]. However, while desirable in the engineered setting, such reactivity is often undesirable in natural systems. Certain ENMs have, for instance, been shown to be toxic to biological organisms [4, 5, 6, 7]. As such, predicting NM fate and transport is essential to understanding their presence in the environment and their threat to humans and other organisms.

It is inevitable that ENMs will be released to the environment during their lifespan either during manufacture, use, or disposal. Aquatic environments are of particular interest because they serve as catchments for industrial, municipal and storm water runoff. They also serve as a drinking water supply and an ecosystem for

countless aquatic species. As stated above, some pristine NMs are known to be toxic to organisms. In addition, NMs can undergo transformations in the environment that impact their fate, transport, and toxicity. Transformations can be chemical (e.g., redox, dissolution), physical (aggregation), biologically-mediated, or via interactions with macromolecules [8]. This work focuses on characterizing physical transformations (specifically, homoaggregation) of NPs based on characteristics of the particle (engineered coatings) and interactions with macromolecules.

1.2.Problem Statement

Because of the vast numbers of ENMs being produced, it is essential to understand the fate and transport of NMs in the natural environment. Due to the wide variety of NM types, finding patterns in NM behavior related to general NM characteristics will help predict behavior in unstudied NMs. Nanoparticle aggregation state is of significance because NP aggregates differ from lone NPs in transport and reactivity. NOM has been observed to impact aggregation between ENMs, and engineered NP coatings have been noted to influence aggregation and interactions between NPs and NOM. In order to gain a fuller understanding of the impact of NOM and engineered coatings, a more in-depth study is needed.

1.3.Significance

Finding patterns in aggregation behavior based on NP characteristics is necessary in order to predict the behavior of unstudied NMs. Determining the aggregation state of NMs is highly significant. Particles that have aggregated are more likely to settle out of solution. NP-NP aggregation due to electrostatic

destabilization can imply a greater propensity for adsorption to or deposition on other materials. As particle size increases, the surface area to volume ratio decreases, meaning less surface area is available for reaction. Reactivity changes can be significant in terms of NM toxicity.

1.4.Objectives

The overarching goal of this study is to improve our understanding of the influence that engineered coatings and NOM concentration have on NP aggregation behavior. The study builds on previous work by Nason and co-workers [9, 10]. The specific objectives of this study were to:

1.) Determine and compare the intrinsic properties of gold NPs stabilized with different capping agents.
2.) Examine the influence of the engineered coatings on aggregation behavior in monovalent and divalent electrolytes.
3.) Examine the effect of NOM on the stability of the NPs in monovalent and divalent electrolytes.

1.5.Approach

This work focused on the stability of two gold NPs (AuNPs) with a core size of ~12 nm: one with an electrostatically-bound citrate multilayer and one with a covalently-bound PEG chain and carboxyl functionality. Particle aggregation was investigated at constant pH under environments of increasing ionic strength for two electrolytes: KCl (monovalent) and $CaCl_2$ (divalent). Suwannee River Natural Organic Matter served as the NOM.

Investigations were carried out as laboratory experiments. Aggregation studies were conducted using dynamic light scattering to determine the relative stability of the NMs in environments of varying ionic strength in the absence and presence of SRNOM. Electrophoretic mobility measurements of NPs in the presence of each electrolyte with and without NOM were used as a quantification of surface charge (and resulting electrostatic repulsive force) of the NPs at each condition. Aggregation studies at a range of ionic strengths and NOM concentrations were performed in the presence of $CaCl_2$ to further investigate the effects of NOM-ion bridging.

The remainder of the thesis is divided as follows: Chapter 2 contains general information regarding the physical transformations of NMs in aquatic environments, including aggregation, NOM adsorption, and the influence of the presence of engineered coatings. Chapter 3 outlines the materials and methods used for the laboratory investigations. Chapter 4 contains results from the laboratory investigations and accompanying discussion. Chapter 5 presents a synopsis of results, implications, broader context for the meaning of the results, and recommendations for future work. Appendix A contains a published manuscript based in part on data generated by the author prior to the investigations presented in this thesis.

Chapter 2: Literature Review

2.1.Physical Transformations

Physical transformation refers to nanoparticle-nanoparticle aggregation, aggregation with other particles, or deposition. These processes occur when particle surfaces come into close proximity and short-range thermodynamic attraction leads to direct particle attachment [11]. Aggregation of like NPs is termed homoaggregation, whereas aggregation of dissimilar particles is heteroaggregation. In both cases, the NM surface area to volume ratio is reduced. The surface area to volume ratio is an integral feature of NMs, which display unique properties and reactivity compared with similar materials of a larger size [2, 3, 12]. When particles aggregate, it limits the effect of size on reactivity. Aggregation also affects NM transport, sedimentation, uptake by organisms, and toxicity [8]. Particles of larger sizes have slower diffusion coefficients and settle out of solution more quickly. Aggregation is hugely important to toxicity, as particle-particle adhesion may affect the mechanisms which allow NPs to gain entry to a cell [13]. While most NPs will aggregate over time, their propensity to do so is affected by several factors.

2.2.Electrostatic Forces

2.2.1. Introduction

Most particles in water exhibit a surface charge (typically negative). In the liquid immediately surrounding a particle, there is a relatively high concentration of ions of the opposite charge due to their attraction to the surface. With increasing distance from the particle, concentrations of counter-ions and co-ions equilibrate with

the bulk solution. This region of relative counter-ion excess is known as the electrical double layer (EDL) [14]. The EDL exists in two parts. The inner region, where ions are specifically adsorbed to the surface, is the Stern layer. Beyond that is the diffuse layer, where ions are less-strongly associated with the particle. Within the diffuse region is a sub-layer termed the shear layer. This defines the boundary between ions that move freely in solution and those which move in conjunction with the particle. The electrical potential at the shear layer boundary is called the zeta potential (ζ). As particles approach one another, their EDLs begin to overlap, resulting in an even higher concentration of counter-ions in the space between the particles. This creates a repulsive force. A certain amount of energy is required to overcome this barrier to achieve particle-particle contact. In this way, the EDL helps to maintain particle stability.

2.2.2. DLVO Theory

In aqueous suspensions, NM stability has been modeled using DLVO (Derjaguin-Landau-Verwey-Overbeek) theory, which is commonly used to describe general colloidal stability. DLVO theory poses that aggregation is a function of the attractive (V_a) and repulsive (V_r) forces between two colloids. Summing these forces gives the total interaction energy (V_t). In classical DLVO theory, attractive forces are dominated by van der Waals attraction and the EDL interactions dominate repulsion [11].

Certain environmental factors can alter the magnitude of attractive/repulsive forces, leading to changes in V_t and the resulting particle stability. The surface charge

of particles, and thus the magnitude of the EDL charge, is affected by pH through either acid/base reactions of surface groups (e.g., surface oxides or acid/base groups) or specific adsorption of protons or hydroxyl ions. The pH at which zeta potential is zero is referred to as the isoelectric point and indicates the point at which electrostatic forces are at a minimum [15]. The surface charge may also be influenced by the adsorption of charged ions or polymeric species.

The ionic strength of an aquatic environment also influences the repulsive force by affecting the thickness of the electrical double layer. At higher ionic strengths, the double layer is compressed due the increased concentration of counter-ions in solution. Thus, the distance at which the repulsive force arises between two particles decreases. At shorter distances, the influence of van der Waals attractive forces increases. Consequently, the overall energy barrier is reduced, tending towards attraction. The ionic concentration at which the repulsive force is minimized is termed the critical coagulation concentration, or CCC [15]. Below the CCC, aggregation is referred to as "reaction-limited," where two particles must approach one another with enough kinetic energy to overcome the energy between the two particles. Above the CCC, the energy barrier is eliminated and aggregation is termed "diffusion-limited." Here, the rate of aggregation is controlled by the rate at which particles diffuse toward one another.

2.3.Steric Forces

In addition to van der Waals and EDL forces, other factors can influence NM stability, including steric forces. When a polymer or polyelectrolyte coating is

adsorbed onto the surface of a particle, it creates a barrier that physically prevents particles from coming into direct contact [16]. Jiang and Oberdörster found that PEG, PEG–NH_2, and PEG–COOH coated quantum dots were stable in a physiological saline solution [17]. In another example, polyvinylpyrrolidone (PVP) coatings on AuNPs provided steric stability that resulted in decreased aggregation [9].

At times, functional groups on the surfaces of these polymer coatings will interact with groups on the surfaces of other NMs. These interactions may be reversible depending on solution chemistry [11, 18]. Determining the potential for reversibility in aggregation is highly important in understanding variability in future fate, transport, and environmental effects of NMs.

2.4.Natural Organic Matter

Natural organic matter (NOM) is a general term that is used to describe broken down organic matter that comes from the degradation of plants and animals. Chemical structures of NOM are complex and variable, but usually involve a high carbon content with a combination of humic and fulvic substances. Fulvic acids differ from humic acids in that they have lower molecular weights and higher oxygen contents. The structure of both humic and fulvic acids generally consist of many phenolate groups and carboxyl functionalities. The propensity of NOM to coat other materials results in it being a controlling factor in determining colloid stability in natural systems and also in determining coagulant dose for particle removal in drinking water treatment [19].

Interactions between NMs and NOM can have several impacts on particle aggregation. Many classes of NM are known to be stabilized by NOM adsorption, including metal oxides [20, 21], metals [22, 23, 24], carbon nanotubes [25], latex nano-colloids [26], and quantum dots [27]. When NOM adsorbs directly to NM surfaces, it stabilizes NPs by imparting additional electrostatic and steric forces [28, 29]. In cases where NOM adsorbs to the surface of NMs that have been stabilized with engineered capping agents, the NMs take on electrochemical characteristics of that class of NOM instead of the characteristics provided by the engineered coating [9].

The presence of divalent electrolytes can cause rapid aggregation of NOM-coated NMs [9, 30, 31, 32, 33, 34]. This increased aggregation between NMs has in part been attributed to a NOM-ion bridging effect. It has been well-documented that NOM interacts specifically with certain divalent electrolytes through complexation reactions [15, 35]. Ions can complex with NOM that has adsorbed to a NP surface, creating a "bridge" that allows for aggregation without core-to-core adhesion. Complexes between NOM and calcium (Ca^{2+}) have been found to result in agglomerates large enough to cause significant fouling to membrane filters, and fouling of a thin-film composite nanofiltration membrane was found to be dependent on Ca^{2+} concentration [36].

Although it has been established that NOM-ion complexes can form bridges between nanomaterials, aggregating particles without core-to-core contact, research in this area is preliminary. Evidence of specific ion bridging between Suwannee River

Humic Acid (SRHA) and calcium ions, Ca^{2+}, have been observed to influence aggregation with a range of nanomaterials [28, 9, 37]. Specific bridging with Ca^{2+} also occurs with alginate, but does not occur with fulvic acid [28, 38]. SRHA also associates specifically with Sr^{2+} and Ba^{2+} ions [39] but does not associate with Mg^{2+} ions [34]. While the aforementioned studies have observed bridging under specific environmental parameters (e.g., specific Ca^{2+} and NOM concentrations), a broader knowledge of aggregation in the presence of bridging components is needed. Varying concentrations of NOM and an electrolyte could, for instance, impact the formation of the NOM-ion complex and therefore NP-NP bridging.

2.5.Engineered NM Coatings

Coatings, or capping agents, are a prevalent accessory to ENMs. These are charged species, ligands, or polymers that are attached to the exterior of a NM. In early research, coated silver-NPs were found to be more stable than uncoated silver-NPs when introduced to the same environmental conditions (ionic strength, pH, and electrolyte type) [40]. NPs with engineered coatings are increasingly being produced in order to provide stability to otherwise highly reactive NP surfaces.

Capping agents can bestow unique chemistry to NPs with similar core structures. NP caps can be engineered to adhere to specific proteins or maintain suspensions at a specific pH. This allows for NPs with the same core structure to be used for a range of applications [40]. Differences in capping agent chemistry, such as the charge of surface functional groups, have been shown to impact NP toxicity [41, 42]. Preliminary evidence shows that engineered capping agents also influence the

stability of NMs in the environment differently. Compared with caps that provide electrostatic stability, caps which stabilize NPs through steric forces provide stability over a greater range of ionic strengths in mono and divalent electrolytes [9].

The combined effects of natural and engineered coatings have been studied previously, and it has been shown that the presence of both factor into NP aggregation behavior [9]. When engineered coatings provide electrostatic stability, effects of ionic strength and electrolyte valence greatly influence NM aggregation. In such cases, the presence of NOM provides additional electrostatic and steric repulsion. When steric stability is provided by an engineered coating, significantly less, or no, aggregation is observed, even in the presence of multivalent electrolytes. Evidence shows that sterically stabilized NPs will aggregate in the presence of some forms of NOM and certain divalent electrolytes, likely via the NOM-ion bridge phenomenon. However, as stated above, this behavior has not been investigated thoroughly.

Chapter 3: Materials and Methods

3.1.Nanoparticles

Gold nanoparticles (AuNPs) were selected as the model NP for this study. Because of their ability to absorb and scatter light with great efficiency, AuNPs are utilized in applications such electronics, cancer treatment therapy, drug delivery, and detection technologies [43, 44, 45, 46]. Due to their popularity in consumer technology and research, AuNPs are available in a variety of well-characterized sizes and surface functionalities.

AuNPs with two different stabilizing agents were investigated. 11 nm AuNPs with an electrostatically bound citrate multilayer (citrate-AuNPs) were purchased from NanoComposix, Inc. AuNPs with a 15 nm core and a covalently bound 3000 Da PEG chain with a carboxyl end-group (carboxyl-AuNPs) were purchased from Cytodiagnostics , Inc. These stabilizing agents were chosen because they exhibit similar carboxyl end-group functionality but have a different mechanism of binding to the gold core (electrostatic vs. covalent). It was also initially hypothesized that the PEG chain could contribute steric stabilization to the carboxyl-AuNPs. The chemical structure of the two functional groups are reported in Figure 1. Average hydrodynamic diameter (D_h) as measured by dynamic light scattering (DLS) in distilled deionized (DDI) water (Barnstead DDI) was 20.2 ± 3.1 nm (95% CI, n = 10) for the citrate-AuNPs and 34.5 ± 0.8 nm (95% CI, n = 10) for the carboxyl NPs. Larger sizes seen with DLS measurements are likely due to the thickness of the capping agent layer surrounding the NP core or due to minor aggregation in the stock

solution. PEG coatings can range in length depending on the morphology of the polymer, i.e., whether the PEG chain is fully-extended or coiled. For a 3000 Da PEG chain, length can range from 4.4 to 23.9 nm, depending on the coil structure of the polymer [47]. The difference in the TEM diameter and hydrodynamic diameter for the carboxyl-AuNPs indicates a PEG length of approximately 9.8 nm, suggesting that PEG chains are intermediately coiled.

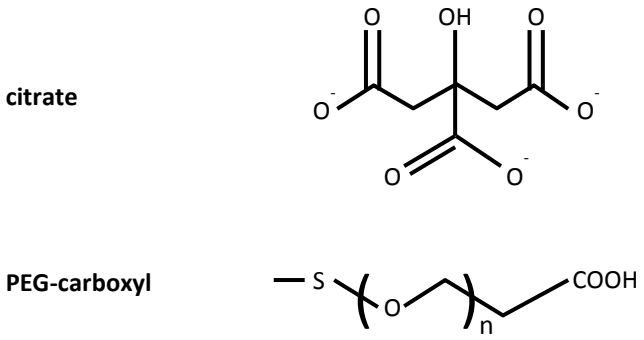

Figure 1. Molecular structures of the capping agents used to stabilize gold nanoparticles, including an electrostatically-bound citrate miltilayer (citrate-AuNP) and covalently-bound PEG chains with a carboxyl end-group (carboxyl-AuNP).

3.2.Suwannee River Natural Organic Matter

Suwannee River Natural Organic Matter (SRNOM) was chosen as the model natural organic matter. SRNOM is a whole water NOM extract isolated by reverse osmosis. Certain fractions of SRNOM, Suwannee River Humic Acid (SRHA) and Suwannee River Fulvic Acid (SRFA) have been used extensively to study the effects of NOM. SRNOM was purchased from the International Humic Substances Society (IHSS). A stock SRNOM solution was prepared by dissolving the lyophilized powder in DDI water to a concentration of 40 mg total organic carbon (TOC)/L at pH 4, as recommended by IHSS. The solution was allowed to stir for 24 hours in the dark and

then filtered through a 0.2 μm nylon membrane filter. Final TOC concentration was assessed using a Shimadzu TOC-VWS (EPA Method 415.1). The SRNOM stock solution was stored in the dark at 4 °C.

3.3.Electrolyte Solutions

All inorganic salts were ACS reagent-grade. Stock solutions were prepared for each salt at a concentration of 1 M and filtered through a 0.2 μm filter.

3.4.NP-NP Aggregation Measurements

AuNP aggregation was quantified by monitoring the change in intensity-weighted hydrodynamic diameter (D_h) over time using time-resolved dynamic light scattering (TR-DLS) with a Brookhaven Instruments 90 plus particle size analyzer. Aggregation of 1 mg/L citrate-AuNPs and carboxyl-AuNPs was measured in the presence of KCl (0-400 mM) and $CaCl_2$ (0-25 mM) with and without the presence of 1 mg C/L as SRNOM at a pH of 5-6 and temperature of 25 °C. For each condition, NPs were added first to a particle free cuvette containing DDI water. When applicable, SRNOM was then added to the cuvette. The cuvette was inverted and allowed to briefly equilibrate before checking pH. Initial particle size was measured with three 1-minute runs and data from these runs was combined for a single initial diameter. After initial sizing, the electrolyte (KCl or $CaCl_2$) was added to the solution. The cuvette was inverted once before quickly initiating the measurement series. D_h was measured at 15 second intervals for 32 min. In order to explore the concentration effects of SRNOM in a solution with a divalent electrolyte, aggregation studies with 1 mg/L carboxyl-AuNPs, 0-10 mg C/L as SRNOM, and 0-500 mM $CaCl_2$ were performed.

Beyond 500 mM, $CaCl_2$ concentrations are environmentally irrelevant for fresh water and brackish water [48, 49]. Finally, to further investigate the nature of SRNOM-Ca^{2+} bonding, several aggregation studies of SRNOM and $CaCl_2$ in the absence of NPs were performed.

The rate of aggregation was quantified using the initial slope of a plot of D_h vs. time (Figure 2). Aggregation rate was then converted to an attachment efficiency using the procedure outlined by Elimelech and co-workers [34, 39]. The initial slope of D_h vs. t is proportional to the absolute aggregation rate coefficient (1).

$$\left(\frac{d(D_h)}{dt}\right)_{t\to 0} \propto k_{11}N_0 \tag{1}$$

where k_{11} is the absolute aggregation rate coefficient between primary particles and N_0 is the initial number concentration of primary particles.

Attachment efficiency, α, is the absolute aggregation rate constant at a particular condition normalized by the aggregation rate constant in the diffusion-limited regime, $k_{11,fast}$ (2). If initial number concentrations are the same in all aggregation trials, there is no need to calculate the absolute rate constant.

$$\alpha = \frac{k_{11}}{k_{11,fast}} = \frac{\frac{1}{N_0}\left(\frac{d(D_h)}{dt}\right)_{t\to 0}}{\frac{1}{N_{0,fast}}\left(\frac{d(D_h)}{dt}\right)_{t\to 0,fast}} \tag{2}$$

Tabulated data of α vs. electrolyte concentration was used to calculate the CCC (Figure 3).

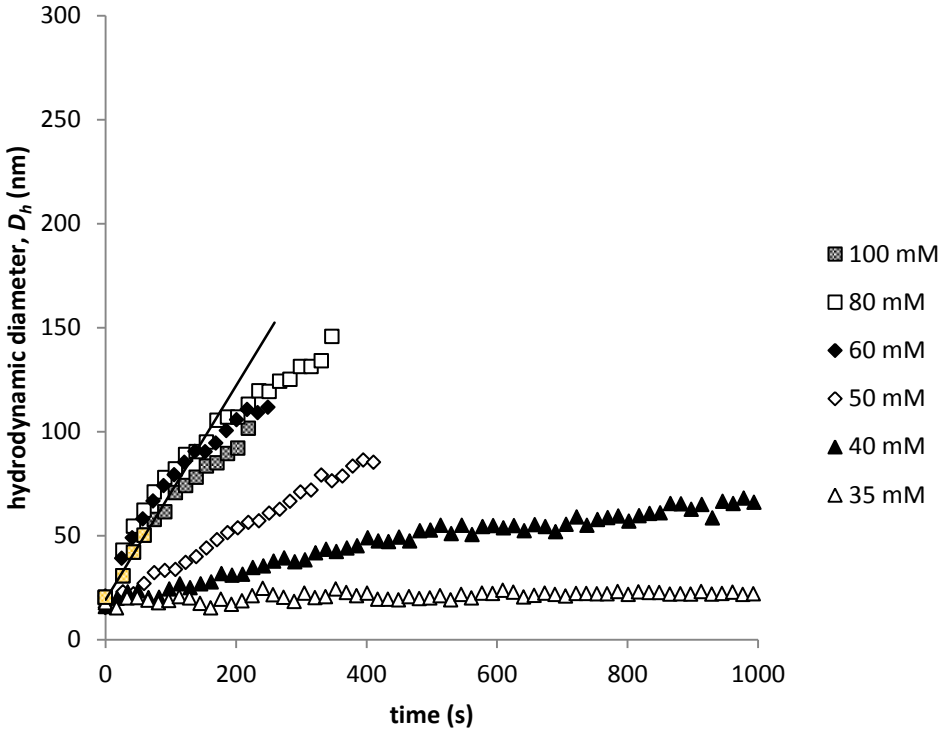

Figure 2. Aggregation of 1 mg/L citrate-AuNPs exposed to increasing concentrations of KCl. Initial aggregation rate was calculated as shown for citrate-AuNP exposure to 100 mM KCl.

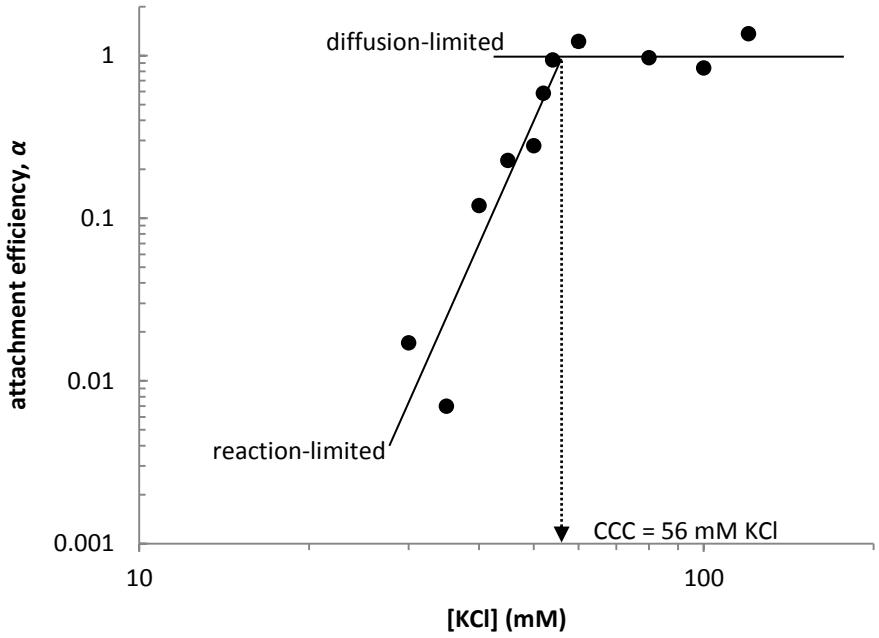

Figure 3. Determination of the CCC for 1 mg/L citrate-AuNPs in KCl is calculated using attachment efficiencies as a function of electrolyte concentration.

The adsorption of SRNOM to NP surfaces was observed to influence the initial rate of aggregation in some cases. As a result, aggregation comparisons were also made using the mean particle size reached after 30 minutes of reaction (averaged over 5 samples bracketing 30 minutes).

3.5.Zeta Potential Measurements

The electrophoretic mobility (EM) of AuNPs was measured using a Brookhaven ZetaPALS instrument. EM for 10 mg/L citrate-AuNPs and carboxyl-AuNPs particles were determined in the presence of 10 mM KCl and 10 mM $CaCl_2$, with and without 1 mg C/L as SRNOM. In order to mitigate the effects of changes in the condition of the electrode with repeated exposure to KCl or $CaCl_2$, the electrode was conditioned in a 0.1 M solution of the appropriate electrolyte prior to experimentation as directed by the manufacturer. All EM measurements were made using a pre-conditioned electrode. Each measurement consisted of the following steps: First, materials were added to a particle-free cuvette of DDI water in the following order: AuNPs, SRNOM, and then electrolyte. Then, pH was checked and adjusted to 6. Finally, cuvettes were allowed to temperature-equilibrate for 2 minutes prior to measurement. For each cuvette, 5 EM measurements were collected and combined for a best-fit analysis using all data points. EMs were converted to zeta potentials (ζ) using the Smoluchowski equation.

Chapter 4: Results and Discussion

4.1. Citrate-AuNPs

As shown in Figure 2 and Figure 3, aggregation of citrate-AuNPs was observed in the presence of the monovalent electrolyte KCl with a CCC of 56.2 mM KCl. Aggregation exhibited DLVO behavior, with low rates of aggregation at low ionic strengths and high rates of aggregation at high ionic strengths. With 1 mg C/L as SRNOM present, aggregation was reduced (Figure 4). A higher concentration of KCl was required to see NP-NP aggregation, reflected in a CCC of 74.3 mM KCl (Figure 5). These changes in aggregation behavior can be explained, in part, by ζ measurements for AuNPs under these conditions. In the absence of SRNOM, ζ for citrate-AuNPs was −7.04 mV, whereas in the presence of SRNOM it was −24.16 mV. A more negative ζ in the presence of NOM is evidence of adsorption of NOM onto the NP surfaces and indicates an increased electrostatic repulsive force between particles [9]. As a result, higher ionic strengths are needed to induce similar aggregation behavior. It is also possible that some steric repulsion is achieved by SRNOM adsorption to the surfaces of the citrate-AuNPs. It has been found previously that SRNOM stabilizes citrate-AuNPs in KCl, but the mechanisms of the interaction were unknown [10]. Zeta potential and aggregation data reported here illustrate the role of electrostatic interactions in the stability of virgin and NOM-coated citrate-AuNPs.

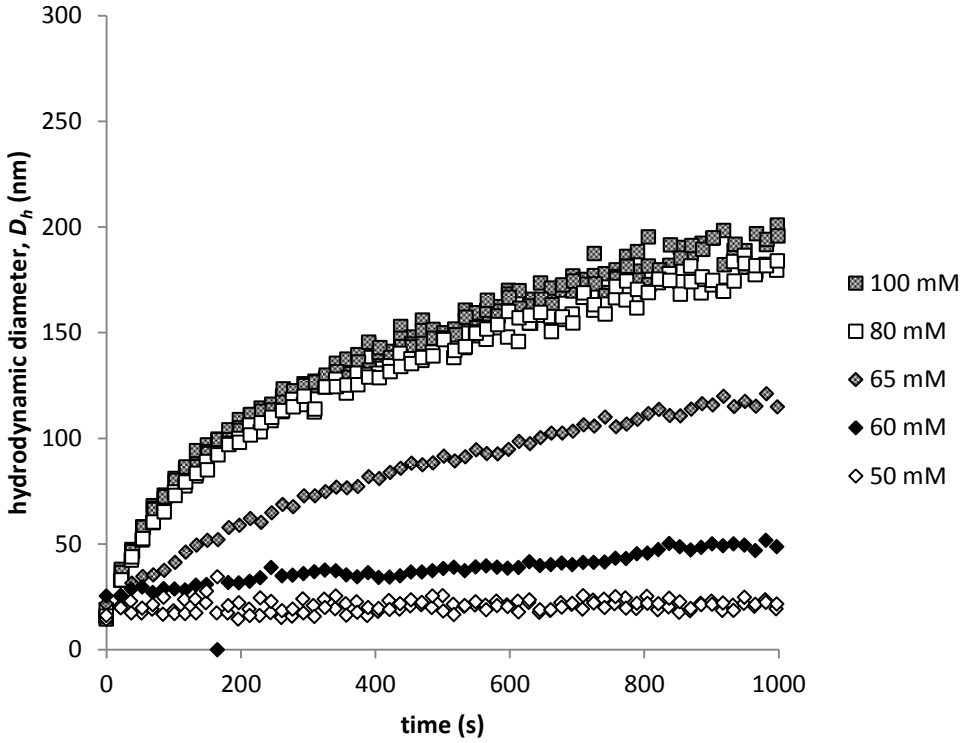

Figure 4. Aggregation of 1 mg/L citrate-AuNPs as a function of time in the presence of 1 mg C/L as SRNOM and increasing concentrations of KCl.

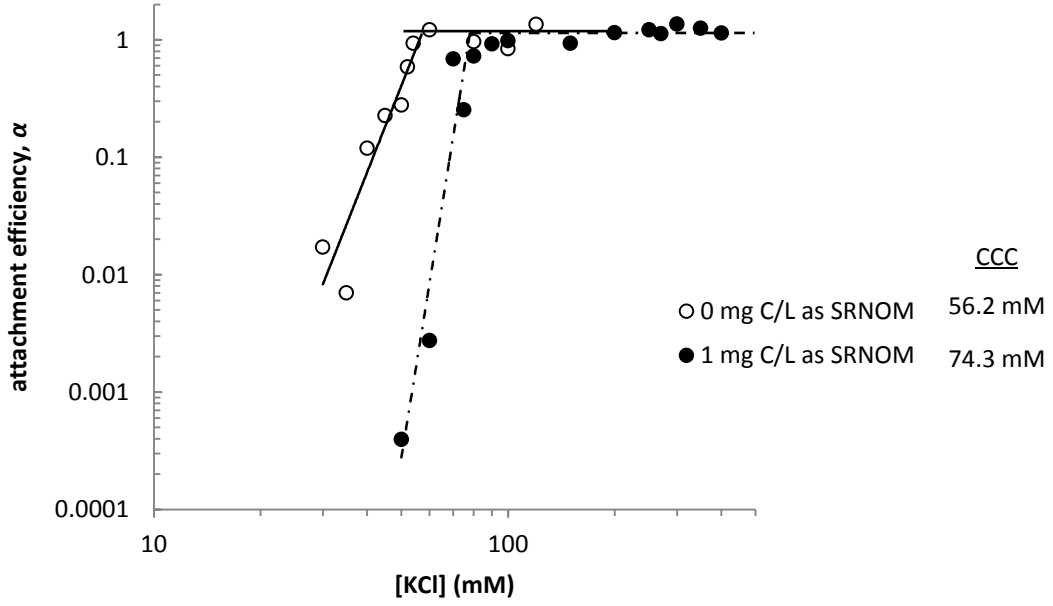

Figure 5. Attachment efficiencies of citrate-AuNPs as a function of KCl concentration in the presence of 0 mg C/L as SRNOM and 1 mg C/L as SRNOM.

Citrate-AuNPs were significantly less stable in the presence of $CaCl_2$ than in the presence of KCl (Figure 6), with a CCC of just 2.28 mM $CaCl_2$ (Figure 7). With divalent ions, the higher density of charge compresses the EDL to a greater extent than with monovalent ions, resulting in a reduced overall repulsive force at the same electrolyte concentration [15]. Zeta potentials for citrate-AuNPs in $CaCl_2$ with and without SRNOM were virtually equivalent (−12.58 mV and −12.88 mV, respectively). It is unclear why the ζ for citrate-AuNPs in 10 mM $CaCl_2$ (without SRNOM) is more negative than the ζ measured in 10 mM KCl. Theory would predict a ζ closer to zero at higher ionic strength.

It has been found that CCC is proportional to NP and solution properties as shown in (3):

$$\mathrm{CCC} \propto \frac{1}{z^6 A_{121}^2} tanh^4\left(\frac{ze\zeta}{4k_B T}\right) \tag{3}$$

where z is electron valence, A_{121} is the Hamaker constant for the particles, e is electron charge, k_B is the Boltzmann constant, and T is absolute solution temperature [16]. For citrate-AuNPs in the presence of electrolyte only, the ratio of CCC_{KCl} to CCC_{CaCl2} was 24.6, whereas the ratio of the functions containing zeta potential and solution condition variables was 0.42. Either a more negative ζ in KCl or a more positive ζ in $CaCl_2$ would be required to match the ratio of CCCs.

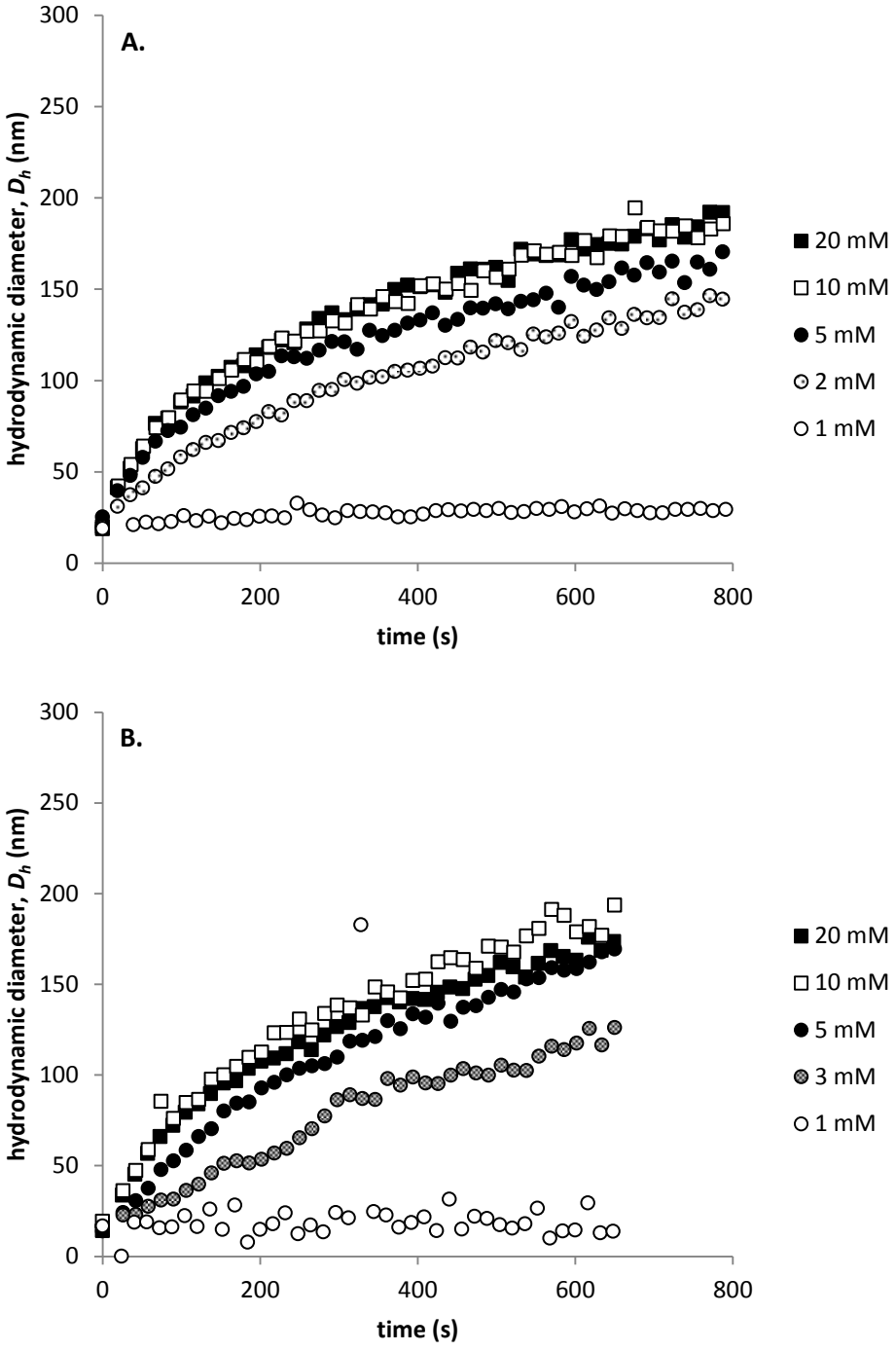

Figure 6. Aggregation of 1 mg/L citrate-AuNPs as a function of time for increasing $CaCl_2$ concentration. (A) in the presence of $CaCl_2$; (B) in the presence of 1 mg C/L as SRNOM and $CaCl_2$.

Only slight stabilization was seen for Citrate-AuNPs in the presence of SRNOM and $CaCl_2$. When attachment efficiencies were compared, particles in 1 mg/L SRNOM aggregated at a slightly slower rate at lower $CaCl_2$ concentrations, but appeared to trend towards marginally higher rates of aggregation at higher concentrations above 4 mM $CaCl_2$ (Figure 7). Higher aggregation rates at higher $CaCl_2$ concentrations were observed with fullerene NPs exposed to SRHA [34].

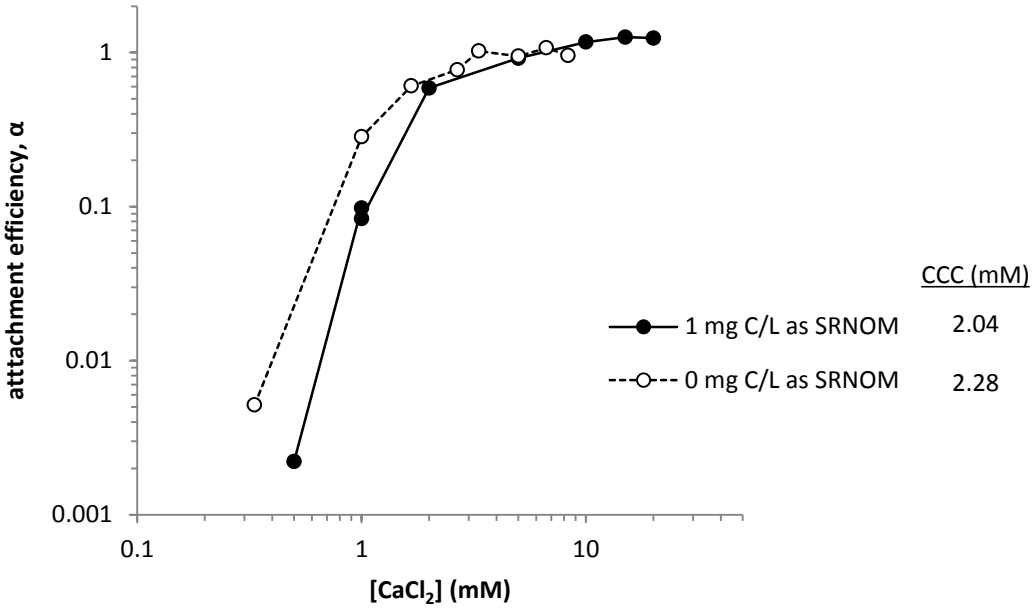

Figure 7. Attachment efficiencies for citrate-AuNPs in the presence of 0 mg C/L as SRNOM and 1 mg C/L as SRNOM. CCC concentrations, in mM $CaCl_2$, are shown in the inset.

Previously, higher rates of NP aggregation in the presence of divalent cations and NOM have been attributed to NOM-ion bridging, where a single calcium ion bonds with functional groups on NOM molecules adsorbed to two different particles, as depicted in Figure 8. NOM-ion bridging was hypothesized to be the source of the increased aggregation of fullerene nanoparticles in the study mentioned above [34]. Stankus, et al. observed higher aggregation rates of citrate-AuNPs in the presence of 5

mg C/L as SRHA and divalent cations [9]. It should be noted that SRHA represents a small fraction of SRNOM. As a higher molecular weight fraction, it is more likely to contribute to bridging. SRFA, the primary component of SRNOM and a lower molecular weight molecule, does not form ion bridges [38]. At the NOM concentrations investigated in this study (1 mg C/L as SRNOM), the concentration of large molecular weight SRHA is quite small. Thus, it is likely that some fraction of SRNOM will participate in bridging activity, but the effect may not be dramatic. The impact of NOM concentration on bridging was further investigated using carboxyl-AuNPs.

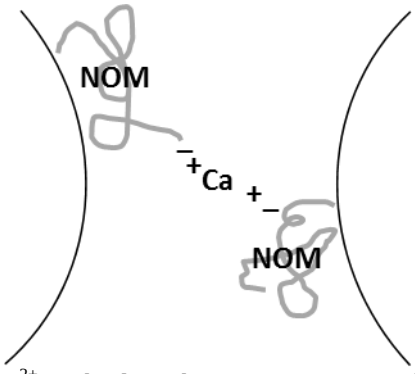

Figure 8. Visual depiction of a Ca^{2+} ion bridging between two negatively-charged NOM species, which in turn are adsorbed to the surfaces of two particles.

4.2.Carboxyl-AuNPs

The aggregation of carboxyl-AuNPs was examined in the presence of KCl concentrations ranging from 0 to 500 mM. No aggregation was seen, even at the highest ionic strengths (Figure 9). The ζ of the carboxyl-AuNPs in 10 mM KCl was −0.98 mV. A ζ close to zero indicates a weakly-charged electrical double layer and a weak electrostatic repulsive force. Because the carboxyl-AuNPs were stable even at high ionic strength, it may be concluded that steric repulsive forces are preventing NP-

NP aggregation. The presence of SRNOM did not influence the stability of the carboxyl-AuNPs in KCl (Figure 9).

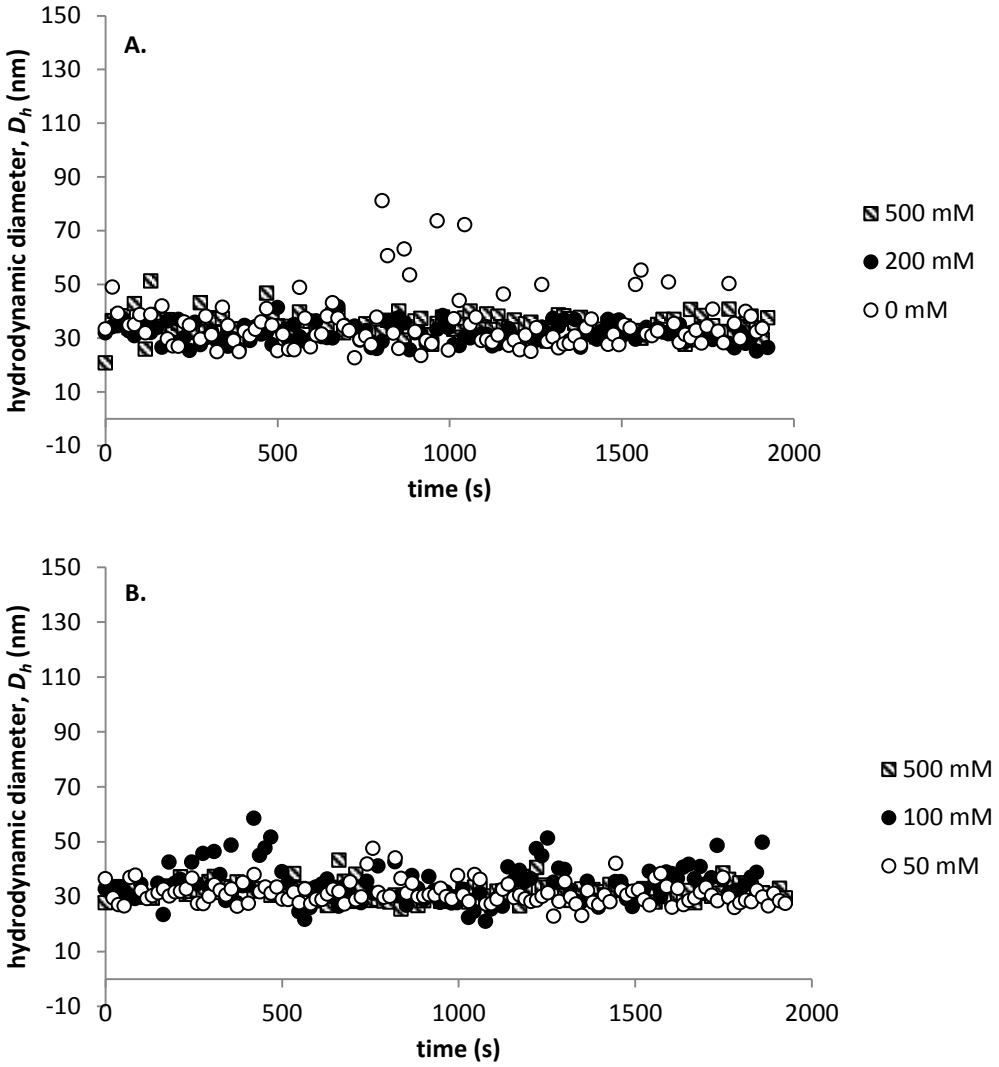

Figure 9. Particle size as a function of time for carboxyl-AuNPs exposed to increasing KCl concentrations. (A) carboxyl-AuNPs with 0 mg C/L as SRNOM. Noise in the 0 mM KCl sample, due to dust, was removed when it exceeded 3 standard deviations of the average size. (B) carboxy-AuNPs with 1 mg C/L SRNOM.

Carboxyl-AuNPs were also stable in $CaCl_2$ concentrations ranging from 0 to 500 mM (Figure 10). No aggregation was observed in TR-DLS trials, and the zeta potential of the carboxyl-AuNPs was −2.08 mV. These ζ values are much smaller in

magnitude than those measured for the citrate-AuNPs. It appears from these results that a citrate multilayer contains a greater charge density than covalently-bound carboxylated chains. This could be influenced by the density of the PEG chains bonded to the surface of the carboxyl-AuNPs and by the greater number of carboxyl groups per citrate molecule (3) than per PEG chain (1).

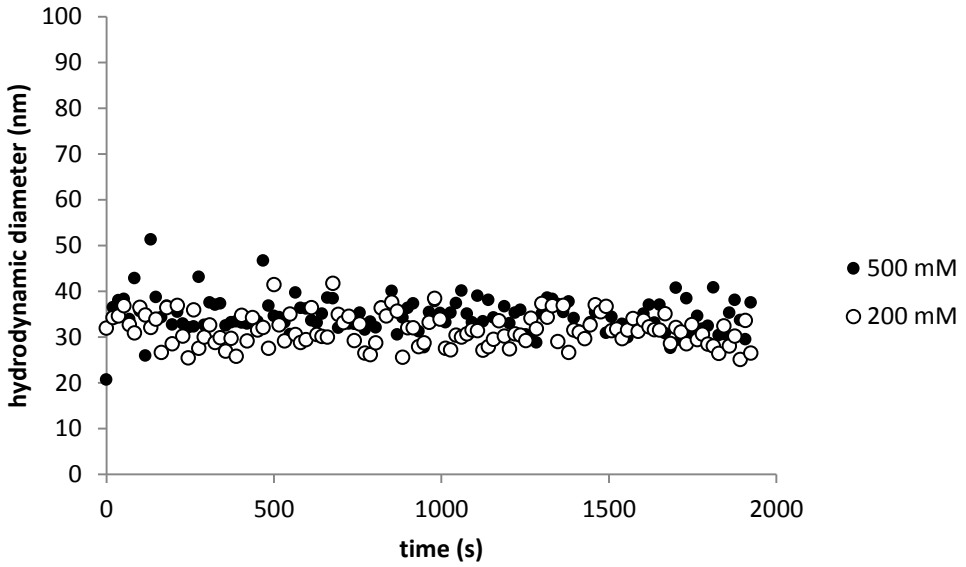

Figure 10. Particle size over time for 1 mg/L carboxyl-AuNPs in several concentrations of $CaCl_2$.

Carboxyl-AuNPs were stabilized by a capping agent that is covalently bonded and able to provide steric stabilization. In Stankus et al., both coatings which provided steric stabilization and those which were attached to the NP core via a thiol bond were found to increase particle stability when compared with other NP caps [9]. Of these two factors, steric stabilization prevented aggregation to a greater degree.

No aggregation, even in the presence of a divalent cation, illustrates the dominance of steric forces over electrostatic forces for these particles. Clearly, the PEG-carboxylate coating is a superior stabilizing agent as compared to citrate. Even

with a more neutral ζ, which indicates electrostatic instability, the carboxyl-AuNPs remained unaggregated. The level of steric stabilization provided by the PEG-carboxylate coating in the presence of $CaCl_2$ is especially significant. Divalent ions are present in most natural waters, and are particularly efficient at electrostatically destabilizing particles.

Additionally, the low ζ of the carboxyl-AuNPs may have contributed to their stability over time. If the low ζ indicates a low density of charged groups, there would be a low likelihood of carboxyl group-Ca^{2+} bridging.

For the carboxyl-AuNPs, the only condition under which aggregation was induced was in the presence of both SRNOM and $CaCl_2$. In this case, particle size increased rapidly for approximately the first 400 s of exposure to $CaCl_2$, after which size increased at a significantly slower rate (Figure 11). This rapid change in hydrodynamic diameter followed by a relatively stable period suggests adsorption of SRNOM to the NPs. Any particle-particle aggregation is reflected in the slower rates of size increase seen over the entire time trial. In Nason et al., the adsorption phenomenon was observed with citrate-AuNPs in a KCl solution with SRHA and Pony Lake Fulvic Acid (PLFA) NOM isolates [10]. Adsorption behavior was also observed for SRFA and SRNOM, but only at high concentrations (5 and 10 mg C/L). With SRHA and PLFA, some aggregation behavior was observed at higher ionic strengths, even when adsorption was thought to be the primary factor influencing D_h. In the case of citrate-AuNPs, it was hypothesized that the NOM was stabilizing the NP by adsorbing either to the exterior of the citrate multilayer or directly to the surface of

the NP core, displacing citrate. In the case of carboxyl-AuNPs, which have covalently-bound functional groups, it is more likely that Ca^{2+} is facilitating SRNOM adsorption by forming a bridge between the NP and the SRNOM. NOM and Ca^{2+} could be interacting directly to the NP core or to the capping agents, depending on capping agent density. The presence of $CaCl_2$ may also promote SRNOM adsorption by changing the conformation of the capping agent PEG chain or the conformation of the SRNOM molecule. A favorable interaction between the carboxyl functionality of the cap, carboxyl groups in the SRNOM, and the divalence of the Ca-cation makes this a likely avenue for the reaction.

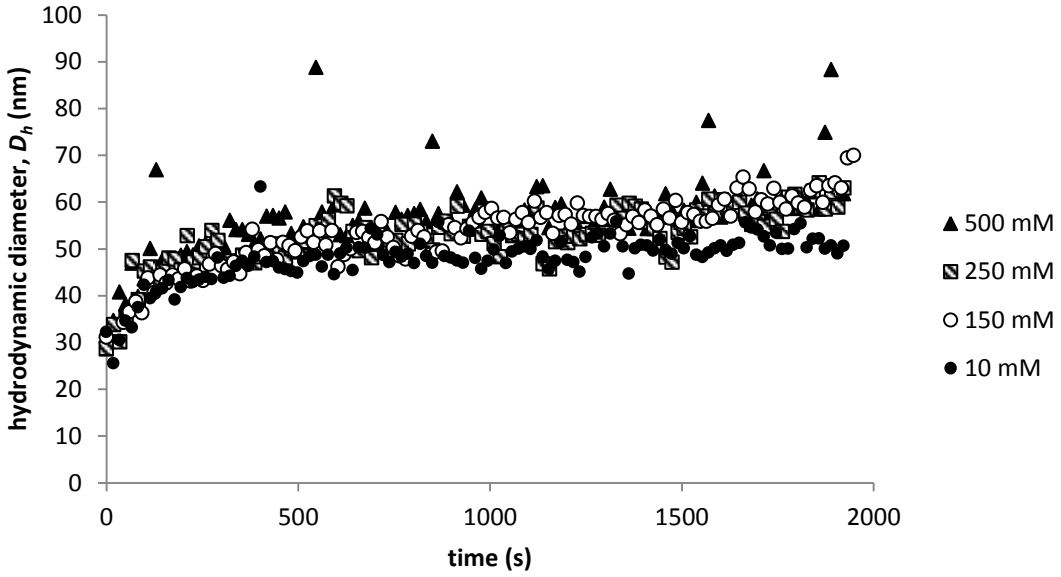

Figure 11. Aggregation behavior of 1 mg/L carboxyl-AuNPs exposed to 1mg C/L as SRNOM and varying concentrations of $CaCl_2$, as noted in the inset.

In Stankus et al., sterically-stabilized PVP-AuNPs only aggregated in the presence of 5 mg C/L as SRHA and 100 mM $CaCl_2$ [9]. No other NOM concentrations were investigated, and it was hypothesized that other concentrations may yield different effects. Because particle size increases were not dependent on

ionic strength at 1 mg C/L (Figure 11), it was hypothesized that SRNOM concentration could be a limiting reactant. To investigate this hypothesis, a matrix of environmental conditions with ranging SRNOM and $CaCl_2$ concentrations were examined; SRNOM concentrations spanned from 0 to 10 mg C/L as SRNOM and $CaCl_2$ concentration was 0 to 500 mM. Carboxyl-AuNP concentration and pH remained constant.

At SRNOM concentrations below 1 mg C/L, TR-DLS curves displayed the trend of particle size increase consistent with adsorption: a rapid increase in D_h followed by a relatively stable particle size. At 5 and 10 mg C/L, particles appear to be aggregating because D_h continues to increase with time rather than reaching a plateau (Figure 12). At 1 and 3 mg C/L, carboxyl-AuNPs displayed a moderate level of aggregation. Initially, these results appear to suggest that there is a relationship between SRNOM and CaCl2 concentrations and aggregation. As SRNOM concentration increases, particle size increases. $CaCl_2$ concentration appears to be a limiting reactant below approximately 150 mM; above 150 mM, D_h at 30 min remains constant for a given SRNOM concentration (Figure 13). In this Experiment, D_h at 30 min was used as a measure of aggregation because it was noted that at 10 mg C/L, SRNOM adsorption to carboxyl-AuNPs resulted in a noticeable increase in D_h even when no electrolyte was present (Figure 14). This behavior impacts the comparison of initial aggregation rates.

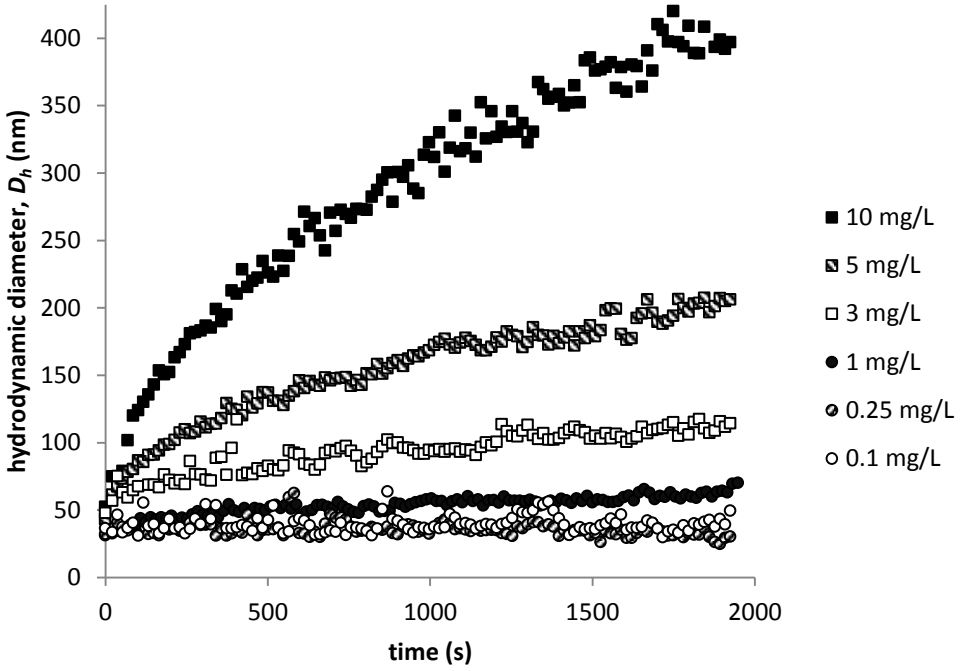

Figure 12. Change in hydrodynamic diameter, D_h, over time for carboxyl-AuNPs in several concentrations of SRNOM (reported as mg C/L) and 150 mM $CaCl_2$.

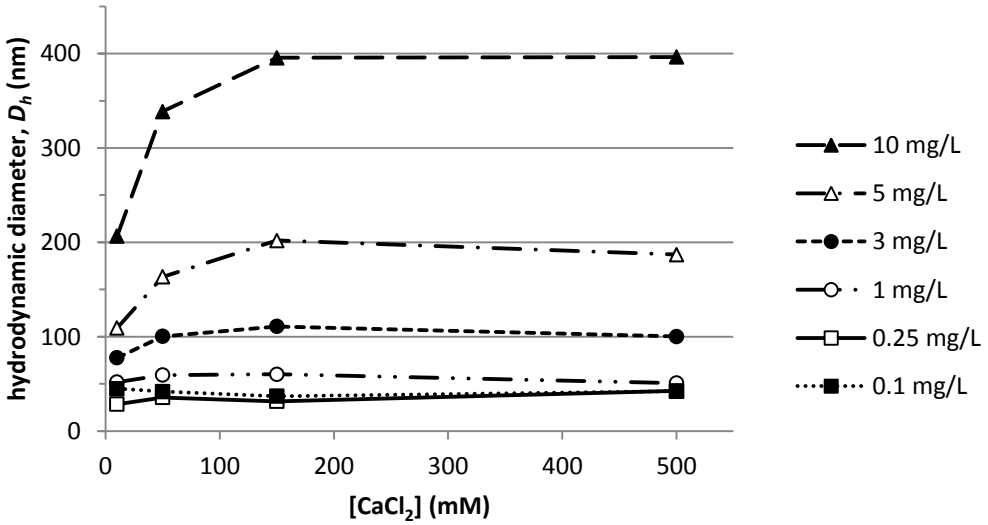

Figure 13. Hydrodynamic diameter of 1 mg/L carboxyl-AuNPs in solutions of several SRNOM concentrations, reported as mg C/L. D_h is reported after 30 min of exposure to $CaCl_2$, as a function of $CaCl_2$ concentration.

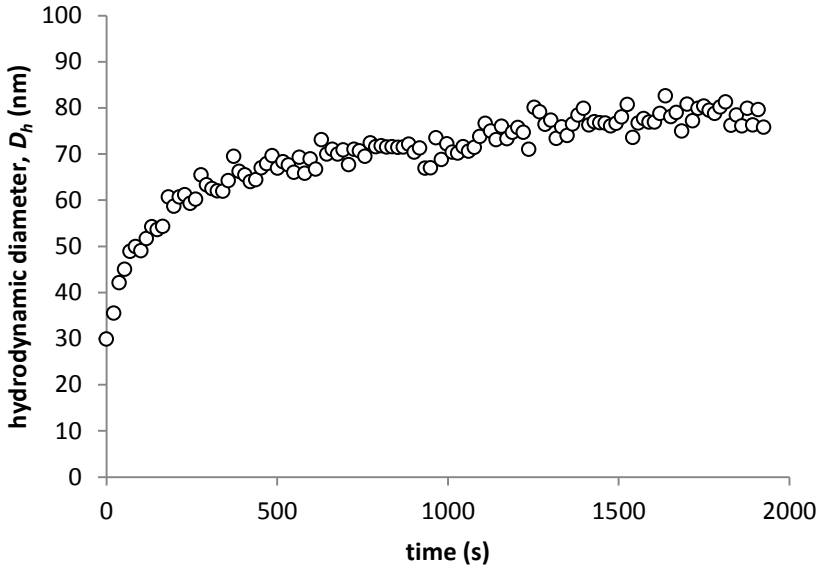

Figure 14. Change in hydrodynamic diameter, D_h, over time for carboxyl-AuNPs in a solution of 10 mg C/L as SRNOM. No electrolyte was present in solution.

In initial efforts to investigate the mechanisms of the interaction between the NPs, SRNOM, and Ca^{2+}, TR-DLS trials of SRNOM in $CaCl_2$ without any NPs were performed. At 1 and 3 mg C/L as SRNOM, no interaction between SRNOM and Ca^{2+} could be observed; DLS consistently returned results with a D_h of 0.0 nm (Figure 15). For these cases, SRNOM aggregation was either not occurring or was occurring at levels undetectable with DLS.

When carboxyl-AuNPs were exposed to 1 and 3 mg C/L SRNOM and $CaCl_2$, aggregation was observed as particle size continued to increase over time (Figure 12). Because aggregation was not observed without the presence of NPs, carboxyl-AuNP size increases can be attributed to NP-NP aggregation facilitated by the presence of SRNOM and $CaCl_2$.

At 5 and 10 mg C/L, aggregation of SRNOM with $CaCl_2$ was observed. When compared with previous data at the same concentrations and 1 mg/L carboxyl-AuNPs,

the trends in D_h with time appeared strikingly similar (Figure 16). This observation makes it difficult to determine whether aggregates observed incorporate NPs or are simply SRNOM aggregates. In the initial seconds of time-resolved D_h measurements, SRNOM in $CaCl_2$ remains undetectable while carboxyl-AuNPs in SRNOM and $CaCl_2$ experience an initial increase in D_h. At these early measurements, it is likely that too few aggregates have formed to be detected.

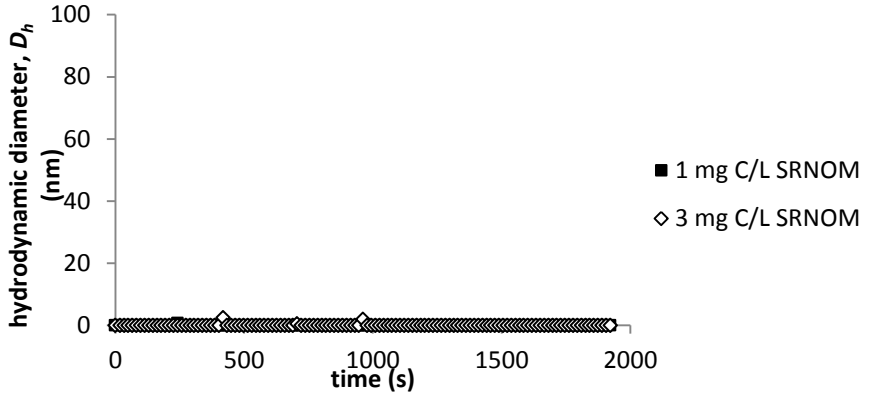

Figure 15. SRNOM size over time in 250 mM $CaCl_2$.

Ion-assisted aggregation of NOM is well-documented [50, 35] and calcium ions have been noted particularly to induce aggregation [51, 52]. Although it is difficult to determine from DLS whether SRNOM aggregates incorporate NPs, the presence of NOM is known to stabilize colloids in solution, presumably by adsorbing to particle surfaces [53, 54]. Recent research has also shown that NOM concentration factors into characteristics of NOM bridging and adsorption. In a recent publication, increasing concentrations of polyacrylamides (PAMs) were found to increase kaolinite floc size in the presence of Ca^{2+} and Mg^{2+} [55]. Around 10 mg PAM/L flocculation reached a plateau or even decreased with increasing PAM concentration. Kaolinite was known to be incorporated in at least a portion the flocculated PAM aggregates due

to measurements of solid-phase PAM and kaolinite concentrations. The current study shows that combined effects of divalent ion concentration and NOM concentration should be considered for NP aggregation.

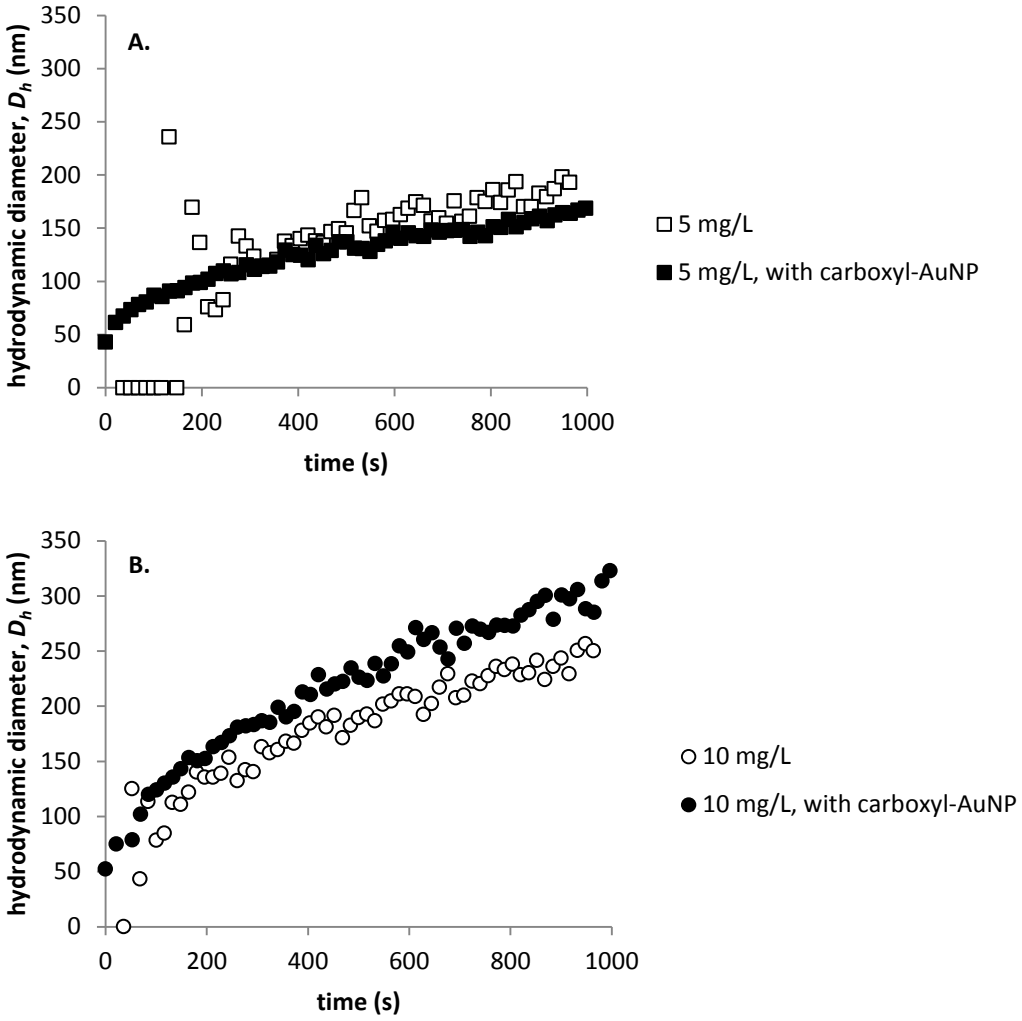

Figure 16. Comparison between TR-DLS runs with and without the presence of carboxyl-AuNPs in a solution of 150 mM $CaCl_2$. (A) compares between trials at 5 mg C/L as SRNOM and (B) compares between trials at 10 mg C/L as SRNOM.

NOM bridging between NPs has been observed by TEM imaging for fullerene and hematite NPs [34, 39]. Different aggregate structures were observed between the fullerene and hematite NPs; bridges between fullerene NPs were comprised of humic

acid and measured up to 100 nm in length while alginate bridges between hematite NPs measured up to approximately one micron. These results suggest that NOM type can greatly influence the bridging structure between NPs. It is also likely that NOM concentration influences bridging structure. In the aforementioned study involving PAM and kaolinite, it was hypothesized that anionic polyelectrolytes and divalent cations can simultaneously induce two types of NOM-ion-particle structures. One type involved PAM bridges between third-party particles (i.e., kaolinite) and the other type occurred when PAM molecules adsorbed completely to one particle, thus stabilizing the particle in solution [55]. The relative presence of these two structures was thought to be dependent on PAM concentration. While this finding sheds light on the potential complexity of NP aggregation in the presence of NOM and divalent cations, further study of AuNPs would be needed in order to determine aggregation/adsorption structures for ENM systems.

Chapter 5: Conclusions

5.1.Key Findings

The following conclusions may be drawn from this work and the supporting literature:

- NPs that are stabilized by a citrate capping agent follow a pattern of aggregation consistent with DLVO theory.
- The citrate multilayer, which provides stabilization primarily through electrostatic repulsion, gained additional electrostatic stability from NOM. Electrophoretic mobility measurements showed that the ζ of citrate-AuNPs in KCl was higher in magnitude in the presence of SRNOM, providing evidence that SRNOM adsorbed to NP surfaces and provided electrostatic stability.
- In $CaCl_2$, SRNOM provided minor stabilization at lower electrolyte concentrations, but appeared to result in slightly greater rates of aggregation at higher concentrations.
- Despite the presence of a greater electrostatic repulsive force, the overall stability of the citrate-AuNPs was inferior to the stability of the carboxyl-AuNPs. Carboxyl-AuNPs remained stable even in the presence of extreme ionic strengths due to steric forces between particles, whereas electrostatically-stabilized citrate-AuNPs were easily destabilized by changes in ionic strength and electrolyte valence. It is likely that other capping agents that sterically stabilize NPs would similarly prevent aggregation. The covalent bond that attached the PEG chain to the gold core may have also contributed some stability to the NP by preventing detachment or displacement of the engineered

coating. The differences in behaviors observed with these two capping agents provide insight into to the spectrum of aggregation behavior that may be seen, with these two NPs representing somewhat extreme cases.

- While NOM provides stability to NPs under some conditions, evidence shows that NOM aggregates in the presence of certain divalent cations (e.g., Ca^{2+}) and can induce aggregation between otherwise stable AuNPs.
- Also evident is that the sizes of aggregates seen with the presence of Ca^{2+} are highly dependent on NOM concentration, and somewhat dependent on the concentration of calcium ions.

5.2.Implications

Differences in aggregation behavior will affect environmental fate, transport and toxicity. Particles that are easily destabilized, as with the citrate-AuNPs, will more readily aggregate and settle, or be filtered out of aquatic systems. NPs that remain stable in solution, such as the carboxyl-AuNPs, will be more likely to remain suspended in an aquatic system and be transported with the flow of water. The types of organisms that come into contact with NPs will differ depending on their location in the natural environment. NP toxicity will in turn depend on aggregation state and NOM adsorption due to changes in exposure and organismal uptake.

Changes in the magnitude of negative charge observed with SRNOM and citrate-AuNPs and the steric stability of carboxyl-AuNPs are highly significant factors when considering the removal of NPs in water treatment processes. Particles with a higher magnitude of negative charge are less likely to be removed by flocculation and

coagulation processes [56]. As mentioned above, unaggregated carboxyl-AuNPs are likely to remain suspended in water. While most NPs can be removed with a nanofiltration membrane, easily-applied removal methods for sterically-stabilized NPs remain unclear at this time.

Strong evidence is provided that adsorption of SRNOM onto sterically-stabilized carboxyl-AuNPs occurs in the presence of Ca^{2+} cations. This adsorption is likely facilitated by NOM-Ca^{2+} complex formation. Recent research has shown that the presence of NOM and divalent ions can both aggregate particles through bridging mechanisms and stabilize particles through layering of adsorbed NOM [55]. The adsorption structure of these complexes to AuNPs is highly important to NP fate and transport. If bridges between NPs are formed, larger NP agglomerates may form. Large NOM-NP agglomerates are more likely to lodge in filtration systems or participate in coagulation/flocculation. If NPs remain relatively small, with one or several layers of NOM adsorbed to their surfaces, transport through aquatic systems is more likely. Stabilized NPs are more likely to remain suspended in open water channels, and SRHA adsorbed to colloid surfaces has been shown to improve transport through the vadose zone [57].

5.3.Further Research

At high SRNOM concentrations, adsorption of SRNOM onto NPs still occurred, but due to the formation of large SRNOM agglomerates, it is unclear how NPs are being incorporated into these larger structures. Previous research has shown that different NOM types and concentrations can affect the size and shape of the

agglomerates produced by NOM bridging between NPs [34, 39, 55]. In the current study, NOM concentration significantly influenced the sizes of aggregates detected. Concentration may also influence aggregate morphology. Investigation by other methods, such as TEM imaging and nanoparticle tracking analysis (NTA) will be necessary to gain insight. TEM would provide good imagery of instances of NP aggregation, and NTA would give a more refined look at particle size distribution over time. However, both of these technologies are limited in terms of sample size. Another option is to investigate with Quartz Crystal Microbalance technology, which is highly effective at determining the affinity of molecules to functionalized surfaces. The affinity of NPs for a surface functionalized with NOM-Ca^{2+} agglomerates could provide new information about the interaction between these groups.

Even though both capping agents displayed carboxyl group functionality, the two engineered coating in this study were drastically different. More subtle patterns in aggregation behavior might be studied by changing the length or density of a sterically-stabilizing capping agent. Also, further examinations of the binding mechanism between the cap and the NP core material could provide novel information.

In this study, pH was kept constant to look into the effects of ionic strength on aggregation of NPs with different capping agents. pH could influence aggregation by affecting the charged state of the engineered coatings or the coating conformation. NOM charge and conformation could also be affected, as could the complexation behavior between NOM and Ca^{2+} ions.

While homoaggregation is a first step towards understanding NP aggregation behavior, environmental concentrations of NPs are so low that they are very unlikely to come into direct contact in the natural environment. Heteroaggregation of NPs with other materials is more likely. Further study into the adsorption of NPs onto NOM-coated surfaces would be highly informative to NP fate and transport models.

The water systems studied in this work, while constructed to approximate natural water systems, do not nearly approach the complexity of actual aquatic environments. It is possible that NP behavior will differ in different environments, and efforts should be made to look into more complex standardized natural waters and actual natural waters.

References

[1] "Nanotechnology Consumer Products Inventory," [Online]. Available: http://www.nanotechproject.org/inventories/consumer. [Accessed 12 July 2012].

[2] M. Auffan, J. Rose, J.-Y. Bottero, G. V. Lowry, J.-P. Jolivet and M. R. Wiesner, "Towards a definition of inorganic nanoparticles from an environmental, health and safety perspective," *Nature Nanotechnology,* vol. 4, pp. 634-641, 2009.

[3] M. F. J. Hochella, S. K. Lower, P. A. Maurice, R. L. Penn, N. Sahai, D. L. Sparks and B. S. Twining, "Nanominerals, Mineral Nanoparticles, and Earth Systems," *Science,* vol. 319, pp. 1631-1635, 2008.

[4] Y.-S. Chen, Y.-C. Hung, I. Liau and G. S. Huang, "Assessment of the in vivo toxicity of gold nanoparticles," *Nanoscale Research Letters,* vol. 4, pp. 858-864, 2009.

[5] Y. Pan, S. Neuss, A. Leifert, M. Fischler, F. Wen, U. Simon, G. Schmid, W. Brandau and W. Jahnen-Dechent, "Size-dependent cytotoxicity of gold nanoparticles," *Small,* vol. 3, no. 11, pp. 1941-1949, 2007.

[6] J. Fabrega, S. R. Fawcett, J. C. Renshaw and J. R. Lead, "Silver nanoparticle impact on bacterial growth: effect of pH, concentration, and organic matter," *Environmental Science and Technology,* vol. 43, no. 19, pp. 7285-7290, 2009.

[7] T. S. Radniecki, D. P. Stankus, A. Neigh, J. A. Nason and L. Semprini, "Influence of liberated silver from silver nanoparticles on nitrification inhibition of Nitrosomonas eropaea," *Chemosphere,* vol. 85, no. 1, pp. 43-49, 2011.

[8] G. V. Lowry, K. B. Gregory, S. C. Apte and J. R. Lead, "Transformation of Nanomaterials in the Environment," *Environmental Science and Technology,* pp. 6893-6899, 2012.

[9] D. P. Stankus, S. E. Lohse, J. E. Hutchison and J. A. Nason, "Interactions between natural organic matter and gold nanoparticles stabilized with different organic cappin agents," *Environmental Science and Technology,* vol. 45, no. 8, pp. 3238-3244, 2011.

[10] J. A. Nason, S. A. McDowell and T. W. Callahan, "Effects of natural organic matter type and concentration on the aggregation of citrate-stabilized gold nanoparticles," *Journal of Environmental Monitoring,* vol. 14, pp. 1885-1892, 2012.

[11] E. M. Hotze, T. Phenrat and G. V. Lowry, "Nanoparticle aggregation: challenges to understanding transport and reactivity in the environment.," *Journal of Environmental Quality,* vol. 39, pp. 1909-1924, 2010.

[12] T. M. Tolaymat, A. M. El Badawy, A. Genaidy, K. G. Scheckel, T. P. Luxton and M. Suidan, "An evidence-based environmental perspectice of manufactured silver nanoparticle in syntheses and applications: a systematic review and critical appraisal of peer-reviewed scientific papers," *Science of the Total Environment,* vol. 408, pp. 999-1006, 2010.

[13] S. J. Klaine, P. J. Alvarez, G. E. Batley, T. F. Fernandes, R. D. Handy, D. Y. Lyon, S. Mahendra, M. J. McLaughlin and J. R. Lead, "Nanomaterials in the environment: behavior, fate, bioavailability, and effects," *Environmental Toxicology and Chemistry*, vol. 27, no. 9, pp. 1825-1851, 2008.

[14] R. J. Hunter, Ed., Foundations of Colloid Science, 2nd ed., New York, NY: Oxford University Press, Inc., 2001.

[15] K. A. Hunter, "Microelectrophoretic properties of natural surface-active organic matter in coastal seawater," *Limnology and Oceanography,* vol. 25, no. 5, pp. 807-822, 1980.

[16] A. R. Petosa, D. P. Jaisi, I. R. Quevedo, M. Elimelech and N. Tufenkji, "Aggregation and deposition of engineered nanomaterials in aquatic environments: role of physiochemical interactions," *Environmental Science and Technology,* vol. 44, no. 17, p. 6532–6549, 2010.

[17] J. Jiang and G. Oberdörster, "Characterization of size, surface charge, and agglomeration state of nanoparticle dispersions for toxicological studies," *Journal of Nanoparticle Research,* vol. 11, pp. 77-89, 2009.

[18] P. Graf, A. Mantion, A. Foelske, A. Shkilnyy, A. Mašić, A. F. Thünemann and A. Taubert, "Peptide-coated silver nanoparticles: synthesis, surface chemistry, and pH-triggered, reversible assembly into particle assemblies," *Chemistry – A European Journal,* vol. 15, no. 23, pp. 5831-5844, 2009.

[19] A. Matilainen, M. Vepsäläinenc and M. Sillanpää, "Natural organic matter removal by coagulation during drinking water treatment: a review," *Advances in Colloid and Interface Science,* vol. 159, no. 2, pp. 189-197, 2010.

[20] A. A. Keller, H. Wang, D. Zhou, H. S. Lenihan, G. Cherr, B. J. Cardinale, R. Miller and Z. Ji, "Stability and aggregation of metal oxide nanoparticles in natural aqueous matrices," *Environmental Science and Technology,* vol. 44, no. 6, pp. 1962-1967, 2010.

[21] S. Ghosh, H. Mashayekhi, P. Bhowmik and B. Xing, "Colloidal stability of Al2O3 nanoparticles as affected by coating of structurally different humic acids," *Langmuir,* vol. 26, no. 2, pp. 873-879, 2010.

[22] S. A. Cumberland and J. R. Lead, "Particle size distributions of silver nanoparticles at environmentally relevant conditions," *Journal of Chromatography A,* vol. 1216, no. 52, pp. 9099-9105, 2009.

[23] R. L. Johnson, G. O'brien, J. T. Johnson, N. Tratnyek and P. G. Tratnyek, "Natural organic matter enhanced mobility of nano zerovalent iron," *Envirnonmental Science and Technology,* vol. 43, no. 14, pp. 5455-5460, 2009.

[24] S. Diegoli, A. L. Manciulea, S. Begum, I. P. Jones, J. R. Lead and J. A. Preece, "Interaction between manufactured gold nanoparticles and naturally occurring organic macromolecules," *Science of the Total Environment,* vol. 402, no. 1, pp. 51-61, 2008.

[25] N. B. Saleh, L. D. Pfefferle and M. Elimelech, "Influence of biomacromolecules

and humic acid on the aggregation kinetics of single-walled carbon nanotubes," *Environmental Science and Technology,* vol. 44, pp. 2412-2418, 2010.

[26] A. J. Pelley and N. Tufenkji, "Effect of particle size and natural organic matter on the migration of nano- and microscale latex particles in saturated porous media," *Journal of Colloid and Interface Science,* vol. 321, pp. 74-83, 2008.

[27] D. A. G. Navarro, D. F. Watson and D. S. Aga, "Natural organic matter-mediated phase transfer of quantum dots in the aquatic environment," *Environmental Science and Technology,* vol. 43, no. 3, pp. 677-682, 2009.

[28] K. L. Chen and M. Elimelech, "Interaction of fullerene (C60) nanoparticles with humic acid and alginate coated silica surfaces: measurements, mechanisms and environmental implications," *Environmental Science and Technology,* vol. 42, pp. 7607-7614, 2008.

[29] L. K. Duncan, J. R. Jinschek and P. J. Vikesland, "C60 colloid formation in aqueous systems: effects of preparation method on size, structure, and surface charge," *Environmental Science and Technology,* vol. 42, pp. 173-178, 2008.

[30] R. F. Domingos, N. Tufenkji and K. J. Wilkinson, "Aggregation of titanium dioxide nanoparticles: role of a fulvic acid," *Environmental Science and Technology,* vol. 43, no. 5, pp. 1282-1286, 2009.

[31] H. Hyung, J. D. Fortner, J. B. Hughes and J.-H. Kim, "Natural organic matter stabilizes carbon nanotubes in the aqueous phase," *Environmental Science and Technology,* vol. 41, no. 1, pp. 179-184, 2007.

[32] Y. Zhang, Y. Chen, P. Westerhoff and J. Crittenden, "Impact of natural organic matter and divalent cations on the stability of aqueous nanoparticles," *Water Research,* vol. 43, p. 42494257, 2009.

[33] A. Franchi and C. R. O'Melia, "Effects of natural organic matter and solution chemistry on the deposition and reentrainment of colloids in porous media," *Environmental Science and Technology,* vol. 37, pp. 1122-1129, 2003.

[34] K. L. Chen and M. Elimelech, "Influence of humic acid on the aggregation kinetics of fullerene (C60) nanoparticles in monovalent and divalent electrolyte solutions," *Journal of Colloid and Interface Science,* vol. 309, pp. 126-134, 2007.

[35] S. Hong and M. Elimelech, "Chemical and physical aspects of natural organic matter (NOM) fouling of nanofiltration membranes," *Journal of Membrane Science,* vol. 132, no. 2, pp. 159-181, 1997.

[36] A. Siedel and M. Elimelech, "Coupling between chemical and physical interactions in natural organic matter (NOM) fouling of nanofiltration membranes: implications for fouling control," *Journal of Membrane Science,* vol. 203, pp. 245-255, 2002.

[37] S.-F. Chen and H. Zhang, "Aggregation kinetics of nanosilver in different water conditions," *Advances in Natural Sciences: Nanoscience and Nanotechnology,* vol. 3, pp. 1-4, 2012.

[38] T. Abe, S. Kobayashi and M. Kobayashi, "Aggregation of colloidal silica

particles in the presence of fulvic acid, humic acid, or alginate: effects on ionic composition," *Colloids and Surfaces A: Physicochemical and Engineering Aspects,* vol. 379, pp. 21-26, 2011.

[39] K. L. Chen, S. E. Mylon and M. Elimelech, "Enhanced aggregation of alginate-coated iron oxide (hematite) nanoparticles in the presence of calcium, strontium, and barium cations," *Langmuir,* vol. 23, pp. 5920-5928, 2007.

[40] A. M. El Badawy, T. P. Luzton, R. G. Silva, K. G. Scheckel, M. T. Suidan and T. M. Tolaymat, "Impact of environmental conditions (pH, ionic strength, and electrolyte type) on the surface charge and aggregation of silver nanoparticle suspensions," *Environmental Science and Technology,* vol. 44, no. 4, pp. 1260-1266, 2010.

[41] S. L. Harper, J. L. Carriere, J. M. Miller, J. E. Hutchison, B. L. S. Maddux and R. L. Tanguay, "Systematic evaluation of nanomaterial toxicity: utility of standardized materials and rapid assays," *ACS Nano,* vol. 5, no. 6, pp. 4688-4697, 2011.

[42] S. Harper, C. Usenko, J. E. Hutchison, B. L. S. Maddux and R. L. Tanguay, "In vivo biodistribution and toxicity depends on nanomaterial composition, size, surface functionalisation and route of exposure," *Journal of Experimental Nanoscience,* vol. 3, no. 3, pp. 195-206, 2008.

[43] D. Huang, F. Liao, S. Molesa, D. Redinger and V. Subramanian, "Plastic-compatible low resistance printable gold nanoparticle conductors for flexible electronics," *Journal of the Electrochemical Society,* vol. 150, pp. G412-G417, 2003.

[44] T. Stuchinkskaya, M. Moreno, M. Cook, D. R. Edwards and D. A. Russell, "Targeted photodynamic therapy of breast cancer cells using antibody–phthalocyanine–gold nanoparticle conjugates," *Photochemical and Photobiological Sciences,* vol. 10, pp. 822-831, 2011.

[45] S. D. Brown, P. Nativo, J.-A. Smith, D. Stirling, P. R. Edwards, B. Venugopal, D. J. Flint, J. A. Plumb, D. Graham and N. J. Weate, "Gold nanoparticles for the improved anticancer drug delivery of the active component of oxaliplatin," *Journal of the American Chemical Society,* vol. 132, pp. 4678-4684, 2010.

[46] S. D. Perrault and W. C. W. Chan, "In vivo assembly of nanoparticle components to improve targeted cancer imaging," *Proceedings of the National Academy of Sciences of the United States of America,* vol. 107, pp. 11194-11199, 2010.

[47] C. Allen, N. Dos Santos, R. Gallagher, G. N. C. Chiu, Y. Shu, W. M. Li, S. A. Johnstone, A. S. Janoff, L. D. Mayer, M. S. Webb and M. B. Bally, "Controlling the physical behavior and biological performance of liposome formulations through use of surface grafted poly(ethylene glycol)," *Bioscience Reports,* vol. 22, no. 2, pp. 225-250, 2002.

[48] J. W. Murray, *Activity Scales and Activity Corrections,* Seattle, WA: University of Washington, 2004.

[49] C. R. Ziegler, G. W. I. Suter, P. J. Kefford, K. A. Schofield and G. J. Pond, "CADDIS Volume 2: Sources, Stressors, and Responses," Environmental Protection Agency, 31 July 2012. [Online]. Available: http://www.epa.gov/caddis/ssr_ion_int.html. [Accessed 11 September 2012].

[50] J. A. Davis, "Complexation of trace metals by adsorbed natural organic matter.," *Geochimica et Cosmochimica Acta*, vol. 48, pp. 679-691, 1984.

[51] A. I. Schäfer, A. G. Fane and T. D. Waite, "Nanofiltration of natural organic matter: removal, fouling and the influence of multivalent ions," *Desalination*, vol. 118, pp. 109-122, 1998.

[52] L. Fan, J. L. Harris, F. A. Roddick and N. A. Booker, "Influence of the characteristics of natural organic matter on the fouling of microfiltration membranes," *Water Research*, vol. 35, no. 18, pp. 4455-4463, 2001.

[53] C. L. Tiller and C. R. O'Melia, "Natural organic matter and colloidal stability: models and measurements," *Colloids and Surfaces A: Physiochemical and Engineering Aspects*, vol. 73, pp. 89-102, 1993.

[54] B. Gu, J. Schmitt, Z. Chen, L. Liang and J. F. McCarthy, "Adsorption and desorption of natural organic matter on iron oxide mechanisms and models," *Environmental Science and Technology*, vol. 28, no. 1, pp. 38-46, 1994.

[55] B. J. Lee, M. A. Schlautman, E. Toorman and M. Fettweis, "Competition between kaolinite flocculation and stabilization in divalent cation solutions dosed with anionic polyacrylamides," *Water Research*, vol. 46, pp. 5696-5706, 2012.

[56] H. Weinberg, A. Galyean and M. Leopold, "Evaluating engineered nanoparticles in natural waters," *Trends in Analytical Chemistry*, vol. 30, no. 1, pp. 72-83, 2011.

[57] V. L. Morales, W. Zhang, B. Gao, L. W. Lion, J. J. J. Bisogni, B. A. McDonough and T. S. Steenhuis, "Impact of dissolved organic matter on colloid transport in the vadose zone: deterministic approximation of transport deposition coefficients from polymeric coating characteristics," *Water Research*, vol. 45, pp. 1691-1701, 2011.

[58] T. Phenrat, Y. Liu, R. D. Tilton and G. V. Lowry, "Adsorbed polyelectrolyte coatings decrease Fe0 nanoparticle reactivity with TCE in water: conceptual model and mechanisms," *Environmental Science and Technology*, vol. 43, no. 5, pp. 1507-1514, 2009.

[59] R. J. Murphy, J. J. Lenhart and B. D. Honeyman, "The sorption of thorium(IV) and uranium (VI) to hematite in the presence of natural organic matter," *Colloids and Surfaces A: Physiochemical Engineering Aspects*, vol. 157, pp. 47-62, 1999.

[60] D. Schmitt, F. Saravia, F. H. Frimmel and W. Schuessler, "NOM-facilitated transport of metal ions in aquifers: importance of complex-dissociation kinetics and colloid formation," *Water Research*, vol. 37, pp. 3541-3550, 2003.

[61] M. Elimelech, J. Gregory, X. Jia and R. Williams, "Surface interacction potentials," in *Particle Deposition and Aggregation: Measurement, Modelling*

and Simulation, Oxford, Butterworth-Heinmann Ltd., 1995, p. 62.

[62] K. L. Chen and M. Elimelech, "Influence of humic acid on the aggregation kinetics of fullerene (C60) nanoparticles in monovalent and divalent electrolyte solutions," *Journal of Colloid and Interface Science,* vol. 309, pp. 126-134, 2007.

[63] T. Abe, S. Kobayashi and M. Kobayashi, "Aggregation of colloidal silica particles in the presence of fulvic acid, humic acid, or alginate: effects of ionic composition," *Solloids and Surfaces: Physiochemical and Engineering Aspects,* vol. 379, pp. 21-26, 2011.

[64] I. Schwyzer, R. Kaegi, L. Sigg, A. Magrez and B. Nowack, "Long-Term colloidal stabiity of 10 carbon nanotube types in the absence/presence of humic acid and calcium," *Environmental Pollution,* vol. 169, pp. 64-73, 2012.

APPENDIX

Effects of Natural Organic Matter Type and Concentration on the Aggregation of Citrate-Stabilized Gold Nanoparticles

Jeffrey A. Nason,*[a] Shannon A. McDowell‡[a] and Ty W. Callahan[b]
DOI: 10.1039/b000000x

The aggregation of 12 nm citrate-stabilized gold nanoparticles (cit-AuNPs) in the presence of four different natural organic matter (NOM) isolates and a monovalent electrolyte (KCl) was evaluated using time-resolved dynamic light scattering. All four NOM isolates stabilized the cit-AuNPs with respect to aggregation. However, specific effects varied among the different NOM isolates. At pH = 6 in 80 mM KCl, low concentrations (<0.25 mg C/L) of large molecular weight Suwannee River Humic Acid (SRHA) was required to stabilize cit-AuNPs, while larger concentrations (>2 mg C/L) of smaller Suwannee River Fulvic Acid (SRFA) were necessary at the same ionic strength. Suwannee River NOM (SRNOM) which contains both SRHA and SRFA behaved in a manner intermediate between the two. Pony Lake Fulvic Acid (PLFA), an autochthonous NOM isolate, provided substantial stability at low concentrations, yet aggregation was induced at NOM concentrations > 2 mg C/L, a trend that is hypothesized to be the result of favourable hydrophobic interactions between coated particles induced at increased surface coverage. For all NOM isolates, it appears that NOM adsorption or conformational changes at the AuNP surfaces result in significant increases in the hydrodynamic diameter that aren't attributable to NP-NP aggregation.

Introduction

New classes of engineered nanomaterials are rapidly being developed and incorporated into consumer goods.[1] Yet, the environmental implications of the potential release of these novel materials into the environment through their manufacture, distribution, use and disposal are largely unknown.[2, 3] It is imperative that the continued development of materials in this booming field be paralleled with detailed study of the environmental implications, including a focus on environmental transport, transformations and fate. The objective of this research was to investigate the roles that natural organic matter (NOM) type and concentration play in influencing the colloidal stability of one class of engineered nanomaterial, citrate-stabilized gold nanoparticles (cit-AuNPs).

It is well established that the adsorption of NOM to the surfaces of natural colloids[4-6] and engineered nanoparticles (ENPs)[7-14] influences, and often controls, surface properties and colloidal stability in natural aquatic systems. Operating in much the same manner, capping agents (charged species, organic ligands, and polymers) are commonly used to tailor nanoparticle properties (*e.g.*, solubility, chemical reactivity, surface chemistry, binding affinity, and colloidal stability). In many instances, the effects of mono- and divalent ions and pH on the stability of ENPs are observed to follow Derjaguin-Landau-Verwey-Overbeek (DLVO) theory where particle stability is controlled by total interaction energy, typically consisting of repulsive electrostatic interactions between like charged particles and attractive van der Waals forces.[15] However, in the presence of NOM and other stabilizing agents, non-DLVO forces including hydrogen bonding, hydration pressure, Lewis acid base interactions, and steric interactions, are also important but not as well understood.[15-17] Various authors have attributed the stability of NOM coated particles (natural or engineered) to enhanced electrostatic[14, 18] and steric[6-8, 14, 19] effects imparted by the NOM coating. In other instances, bridging flocculation of natural colloids and engineered nanoparticles has been seen in presence of NOM[6, 8, 20] and exacerbated when elevated concentrations of divalent cations are present.[7, 21]

A crucial step in the evaluation of NP transport, transformation, toxicity and fate in the environment is a systematic analysis of factors controlling the interactions between NOM and ENPs. Many of the studies cited above have used a single NOM isolate such as Suwannee River Humic Acid (SRHA) to represent NOM. Although tremendously useful as a standardized material, in reality, the character and concentration of NOM

can vary substantially in different aquatic systems. Systematic investigations of the influences of different NOM fractions or NOM from different sources are lacking, although a few recent studies have examined ENP stability in the presence of different NOM isolates[19] or actual water samples.[11, 22, 23] As a result, much remains unknown about (1) what characteristics of NOM influence their interactions with engineered nanoparticles; (2) the influence of NOM concentration; and (3) the mechanisms by which NOM interacts with ENPs (coated and uncoated) and what implications those interactions have for ENP colloidal stability in aquatic systems.

A large body of work indicates that interactions between NOM and ENPs in aquatic systems influence surface chemistry and stability and that those interactions will also influence environmental transport and fate. However, the current paradigm for assessing environmental behavior appears to be a process of testing materials and release scenarios (*e.g.*, dispersion in different aquatic chemistries) one by one. There is a need to take a broader view that will correlate environmental behavior with specific properties of the ENPs and the aquatic chemical composition (including NOM content and character) and to incorporate those findings into predictive models for environmental transport and fate.

In this article, we present the results of time-resolved dynamic light scattering experiments used to quantify the rates of aggregation of cit-AuNPs as a function of ionic strength in the presence and absence of varying concentrations of four different NOM isolates. We discuss the correlation of cit-AuNP aggregation behavior with the physicochemical properties of the different NOM isolates, as well as reporting on the influence of NOM concentration. Additionally, we discuss the results of supporting analyses using small-angle x-ray scattering to shed light on the mechanisms of the NOM-NP interactions.

Materials and methods

Gold nanoparticles

Citrate-stabilized gold nanoparticles (cit-AuNPs) (NanoXact) were purchased from NanoComposix, Inc. (San Diego, CA). As measured by TEM and reported by the manufacturer, AuNP core diameter was 12.0 ± 1.3 nm (1 standard deviation). The average hydrodynamic diameter as measured by dynamic light scattering in distilled deionized (DDI) water was 20.2 ± 3.1 nm (95% CI, n = 10). The difference in the two methods may be partly attributed to the layer of adsorbed citrate ions, although several reports of citrate adsorption onto gold and gold colloids suggest an adsorbed layer thickness on the order of 0.4-0.7 nm[24, 25], not large enough to account for the differences seen here. Another possible explanation is that the NPs were slightly aggregated in the stock solution.

Natural organic matter isolates

Suwannee River Natural Organic Matter (SRNOM), Suwannee River Humic Acid (SRHA), Suwannee River Fulvic Acid (SRFA), and Pony Lake Fulvic Acid (PLFA) were purchased from the International Humic Substance Society (IHSS). Each NOM isolate was dissolved to a concentration of approximately 40 mg/L total organic carbon (TOC) in distilled deionized (DDI) water (Barnstead Nanopure). The NOM solutions were stirred for 24 hr in the dark and then filtered through a 0.2 µm nylon membrane syringe filter (Whatman). The pH of the stock solutions was adjusted to 6.0 with NaOH or HCl as appropriate. Final dissolved organic carbon concentrations of the stock solutions were quantified using a Shimadzu TOC-VCSH total organic carbon analyzer (EPA Method 415.1).

Electrolytes

All inorganic salts were ACS reagent-grade. 1 M stock solutions were prepared for each salt in DDI water followed by filtration through a 0.02 µm syringe filter (Whatman, Anotop 25).

Time-resolved dynamic light scattering

Cit-AuNP stability was studied as a function of ionic strength (KCl) in the presence and absence of the 4 NOM isolates at a concentration of 1 mg C/L. In addition, aggregation was quantified in 80 mM KCl at NOM concentrations varying from 0 to 10 mg C/L. In all aggregation studies, the ambient pH after dispersion was between 5 and 6 and cit-AuNP concentrations were 1 mg/L as Au, unless otherwise noted.

Aggregation of the cit-AuNP suspensions was quantified using time-resolved dynamic light scattering (TR-DLS); the intensity-weighted hydrodynamic diameter (D_h) was measured at 15 s intervals for periods ranging from 10-30 min with a 90Plus particle size analyzer (Brookhaven Instruments, Holtsville, NY). Details of the specific procedures have been reported previously.[21] In short, cit-AuNPs were suspended in DDI water in 3.5 mL cuvettes and the size was checked. Then, the NOM isolate was added and the size was checked again. Finally, electrolyte was added and the cuvette was quickly inverted and placed in the instrument.

Aggregation rates were calculated from the initial slope of a plot of D_h vs. t and converted to attachment efficiencies following the procedure outlined by Elimelech and co-workers.[7, 26-28] The initial slope of D_h vs. t is proportional to the absolute aggregation rate coefficient as shown in Eq. 1) [27]:

$$\left(\frac{d(D_h)}{dt}\right)_{t\to 0} \propto k_{11}N_0 \qquad (1)$$

Where k_{11} is the absolute aggregation rate coefficient between primary particles and N_0 is the initial number concentration of primary particles. The attachment efficiency, α, is the aggregation rate constant at a particular condition normalized by the aggregation rate constant in the diffusion-limited (fast) regime as shown in Eq. 2.[26]

$$\alpha = \frac{k_{11}}{k_{11,\,fast}} = \frac{\frac{1}{N_0}\left(\frac{d(D_h)}{dt}\right)_{t\to 0}}{\frac{1}{N_{0,\,fast}}\left(\frac{d(D_h)}{dt}\right)_{t\to 0,\,fast}} \qquad (2)$$

If the initial number concentrations are the same in all aggregation trials, there is no need to calculate the absolute rate constant.

Tabulated data of α vs. ionic strength was used to calculate the critical coagulation concentration (CCC), the electrolyte concentration at which the energy barrier due to electrostatic repulsion between NPs is eliminated by screening of the surface potential by counter-ions in solution.[29] If aggregation behavior follows DLVO theory, particles will aggregate slowly in a reaction-limited regime at low electrolyte concentrations. In this regime, the aggregation rate increases with increasing electrolyte concentration. However, once the CCC is reached (and the energy barrier eliminated), particles aggregate rapidly at a rate that becomes independent of ionic strength (diffusion-limited regime). Experimentally, the CCC is calculated as the electrolyte

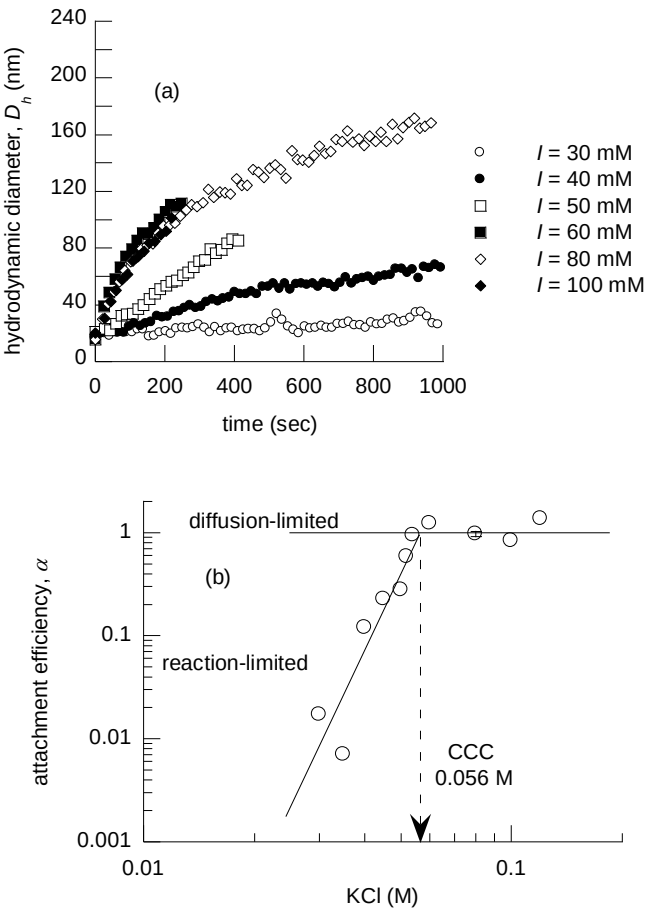

Fig. 1 Aggregation of citrate-stabilized AuNPs in KCl. (a) TR-DLS profiles of Dh for 1 mg/L citrate-stabilized AuNPs in KCl solutions of varying ionic strength. (b) Attachment efficiencies for citrate-stabilized AuNPs as a function of KCl concentration. The CCC calculated from Figure 1b is 56 mM KCl.

concentration where the regression lines extrapolated through the two aggregation regimes intersect. For cit-AuNPs in the presence of the four NOM isolates, initial aggregation rates were converted to attachment efficiencies using the diffusion limited aggregation rate from the cit-AuNPs in KCl without NOM.

Small angle x-ray scattering

Time-resolved small angle x-ray scattering (SAXS) experiments were performed using an Anton Paar SAXSess. cit-AuNP suspensions were prepared in a fixed cuvette as described above and scattering intensity was monitored at 10 s intervals for a period of 1000 s. cit-AuNP concentrations were 10 mg/L for the SAXS trials to achieve suitable scatterin intensities. Scattering data were analyzed using Igor Pro v6.02A software (Wavemetrics, Inc) and the Irena 2 macro[30].

Results and discussion

Ionic strength effects

Aggregation profiles of the cit-AuNPs in varying strength KCl (30-120 mM) are presented in Fig. 1a. In the absence of NOM, the cit-AuNPs exhibit classical DLVO-type behavior. Particles are quite stable at low ionic strengths where a substantial energy barrier exists as a result of electrostatic repulsion between the negatively charged particles (zeta potential = −20 mV at pH = 6 and I = 10 mM[21]). However, as the electrical double layer is compressed by increasing the ionic strength, the rate of aggregation increases until the CCC is reached. Plotting the attachment efficiency against KCl concentration reveals that the critical coagulation concentration is approximately 56 mM KCl (Fig. 1b). These results provide evidence that there is a strong electrostatic component to the stabilization of the AuNPs by the citrate capping agent. Similar results have been reported for the stabilization of TiO_2 NPs by citric acid.[31]

Aggregation data were also collected for 1 mg/L cit-AuNPs suspended in solutions containing KCl (50-450 mM) and 1 mg C/L of each of the four NOM isolates. SRFA and SRHA have been widely used in studies examining NOM effects on colloidal stability and provide a useful point of comparison with previous studies. Only rarely have the effects of these two isolates been compared.[19] SRNOM was chosen to more closely represent NOM character of natural water, but whose effects could also be analysed in reference to its component parts (SRFA and SRHA). SRNOM (as well as SRFA and SRHA) are allocthonous NOM isolates. Finally, PLFA, an autochthonous NOM from a eutrophic lake in Antarctica was chosen because of the contrast in its source and chemical makeup.

Prior to commencing aggregation with the addition of KCl, D_h was measured after equilibration with each NOM isolate as described above. There were no significant differences between the cit-AuNPs in DDI water and the cit-AuNPs in contact with each of the NOM isolates (paired t-tests; α=0.05; n = 10-12 for each condition). These results suggest that if NOM adsorption were taking place at these low ionic strengths, it did not result in a significant change in the initial D_h at the sensitivity detectable by the DLS (95% CIs on the initial diameters ranged from 1.1-3.1 nm).

Aggregation profiles for cit-AuNPs in the presence of the four NOM isolates are shown in Fig. 2. When compared with the results shown in Fig. 1a, Fig. 2a-d reveal that the four NOM isolates stabilized the cit-AuNPs as evidenced by slower rates of aggregation in the presence of NOM at 1 mg C/L, especially at KCl concentrations ranging from 60-100 mM. As with the cit-AuNPs in the absence of NOM, particles are stable at low KCl

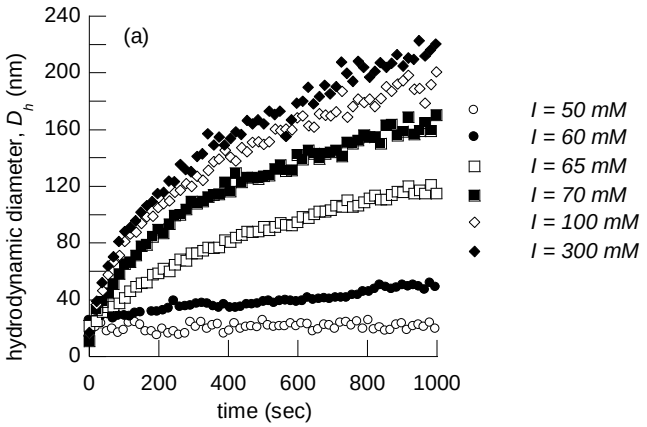
(a)
hydrodynamic diameter, D_h (nm)
240
200
160
120
80
40
0
0
200
400
600
800
1000
time (sec)
I = 50 mM
I = 60 mM
I = 65 mM
I = 70 mM
I = 100 mM
I = 300 mM

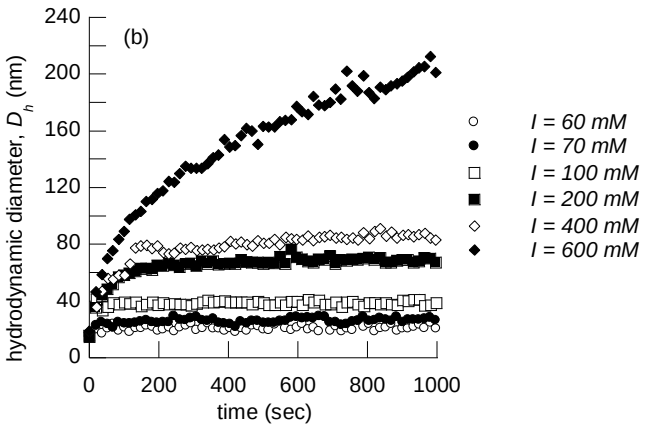
(b)
hydrodynamic diameter, D_h (nm)
240
200
160
120
80
40
0
0
200
400
600
800
1000
time (sec)
I = 60 mM
I = 70 mM
I = 100 mM
I = 200 mM
I = 400 mM
I = 600 mM

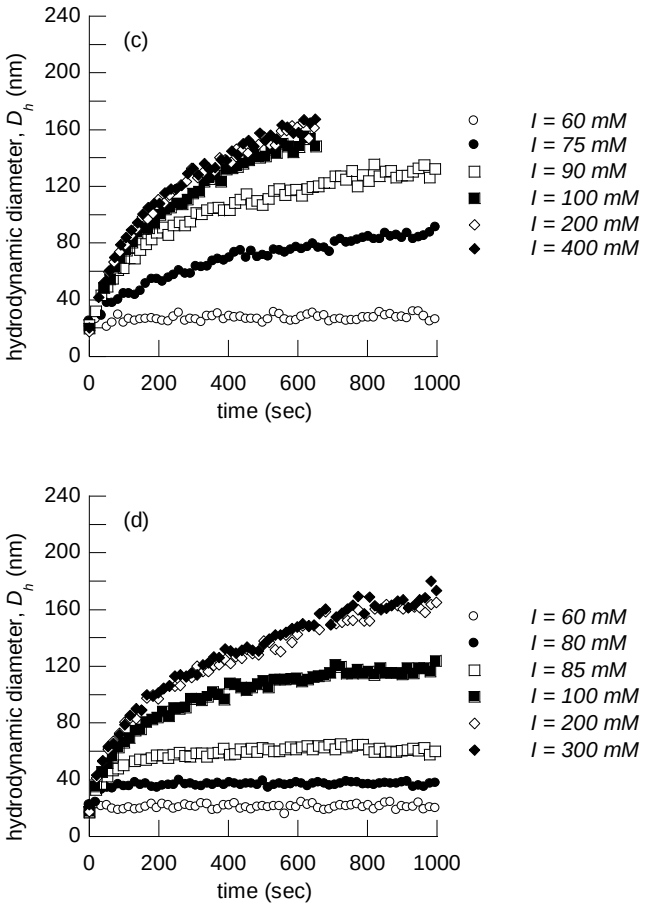

Fig. 2 Aggregation of cit-AuNPs in the presence of NOM isolates and KCl. (a-d) TR-DLS profiles of cit-AuNPs in 1 mg C/L as SRFA, SRHA, SRNOM and PLFA, respectively.

concentrations and aggregation rates increased with increased ionic strength before plateauing.

Attachment efficiencies as a function of KCl concentration are shown in Fig. 3 and the various CCCs are tabulated in the inset. Despite the substantial amount of overlap between the four NOM isolates, it is clear that the CCC for the cit-AuNPs was shifted to higher ionic strengths in the presence of 1 mg C/L as each of the NOM isolates. These results again demonstrate the stabilizing effect of NOM. Furthermore, they indicate that at there is still a strong electrostatic component to the repulsive forces between particles in the presence of the four NOM isolates over the range of ionic strengths investigated. It should be noted that the D_h vs. t profiles of the cit-AuNPs in the presence of SRHA (and to some extent PLFA) were markedly different than for cit-AuNPs in the presence of the other three NOM isolates and calls into question the appropriateness of using a CCC to quantitatively describe aggregation behavior (*vide infra*). Nevertheless, it is clear from Fig. 3 that the cit-AuNPs were stabilized by all four NOM isolates.

Despite similarities in the general trends of NOM-coated AuNP aggregation, the specifics of the aggregation behavior are somewhat different between the four NOM isolates. In the presence of SRFA (Fig. 2a), cit-AuNPs aggregate rapidly at ionic strengths greater than approximately 70 mM. Aggregation is rapid initially and continues at a slowing rate due to the continuous reduction of particle number concentration inherent in all aggregation processes (each NP-NP collision reduces the total number concentration by one).[32] Virtually identical results were seen for SRNOM (Fig. 2c), which is not suprising owing to the fact that SRFA is a primary component of SRNOM.[33]

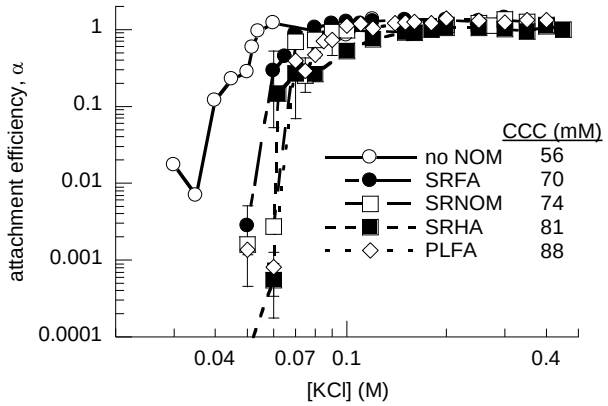

Fig. 3 Attachment efficiencies of AuNPs in the presence of 1 mg C/L of the four NOM isolates. CCC concentrations for AuNPs in each NOM isolate are shown in the inset table.

Comparing the aggregation behavior of cit-AuNPs in the presence of SRFA (Fig. 2a) and SRHA (Fig. 2b) reveal striking differences. Although the D_h of the SRHA coated AuNPs initially increased rapidly at elevated ionic strength, D_h generally leveled off and became relatively stable after approximately 3-5 minutes. For SRHA, D_h did continue to increase after 5 minutes, but at slower rates than the cit-AuNPs in contact with SRFA, which continued to grow rapidly throughout the monitoring period. It wasn't until the ionic strength was increased to > 600 mM KCl that the cit-AuNPs began to aggregate rapidly over the duration of the experiment.

Aggregation profiles for cit-AuNPs in contact with PLFA (Fig. 2d) shared aspects of the characteristics of cit-AuNPs in contact with both SRFA and SRHA. Rates of NP aggregation increased with increasing ionic strength until the CCC was reached, although the CCC was shifted to a higher ionic strength indicating that PFLA is more effective at stabilizing the cit-AuNPs. At ionic strengths ≤120 mM KCl, behavior similar to that of SRHA was seen; profiles were characterized by an initial rapid increase in D_h followed by a relatively stable plateau.

We hypothesize that the the initial change in D_h for cit-AuNPs in contact with SRHA and PLFA is related to changes in NOM conformation or dynamic NOM-AuNP interactions (*e.g.*, adsorption) induced upon the addition of KCl rather than NP-NP aggregation. As has been demonstrated previously, NOM conformation and adsorption to natural colloids and ENPs is strongly influenced by ionic strength. For example, Vermeer *et al.* found that adsorption of purified Aldrich humic acid (AHA) onto hematite nanoparticles increased with increasing ionic

strength.[34] This effect was attributed to reduced intramolecular repulsion between adsorbed AHA molecules. Adsorbed layer thicknesses of approximately 40-50 nm were measured by DLS for the particles coated with the large molecular weight AHA. Franchi and O'Melia showed similar results for adsorption of SRHA on latex NPs, documenting 1-4 nm increases in D_h for the 98 nm particles upon addition of 1 mg C/L as SRHA.[9] Again, the findings were attributed to screening of inter- and intramolecular electrostatic forces between functional groups on SRHA molecules at increased ionic strength, resulting in denser adsorbed layers of more highly coiled SRHA molecules that extended further into solution. Recently, Domingos *et al.* attributed increased stability of TiO_2 NPs at increased ionic strength and pH = 8 to increased SRFA adsorption.[8] However, this behavior was not accompanied by a measurable increase in D_h. On the contrary, D_h decreased with increasing ionic strength, a trend that was attributed to increased SRFA adsorption and an accompanying disaggregation of TiO_2 aggregates via steric stabilization.

In context of these previous findings, it is likely that the rapid initial changes in D_h and the influence of ionic strength seen in Figures 2b (≤ 400 mM KCl) and 2d (≤ 120 mM KCl) are the result of increased NOM adsorption rather than NP-NP aggregation. In the case of SRHA, after the short period of adsorption the SRHA coated partcles were quite stable over a range of ionic strengths suggesting that steric stabilization or other non-DLVO interactions were controlling the interaction energy between particles. This was likely also the case for PLFA at ≤ 120 mM KCl. However, in both cases, the repulsive forces were overcome with continued increases in ionic strength. Examining the D_h after approximately 5 minutes in Fig. 2b and 2d suggests that adsorbed layer thicknesses were approximately 4-30 nm for SRHA and 4-12 nm for PLFA. Although increased adsorption with increased ionic strength is also likely occuring for SRFA and SRNOM, these effects are masked by aggregation of the NOM coated cit-AuNPs and are examined further in the section detailing NOM concentration effects.

To begin testing the above hypothesis, we performed preliminary small-angle x-ray scattering experiments in the presence and absence of SRHA in 80 mM KCl. The advantage of SAXS is that it yields direct insitu measurements of nanoparticle core size.[35] In general, these experiments were performed in the same fashion as the TR-DLS experiments. The size of the cit-AuNPs was initially measured and then tracked over time after the addition of KCl. Plots of scattering intensity and fitted size distributions are shown in the supplementary information (Fig. S1-S4†). Initial size measurements of the cit-AuNPs in DDI water revealed a core size of 12.8 nm, very close to the TEM based core size reported by the manufacturer. In the absence of SRHA, significant aggregation of cit-AuNP were detected in the 15 minutes following KCl addition to 80 mM. However, in the presence of SRHA, the cit-AuNP core size was essentially unchanged (12.4 nm) with some minor aggregation detected. These preliminary results support the hypothesis that SRHA inhibits aggregation of cit-AuNPs, but that D_h changes fairly dramatically due to increased adsorption of SRHA molecules onto cit-AuNPs at elevated ionic strength.

As described in the introduction, the use of organic capping agents to stabilize engineered nanoparticles is widespread. Furthermore, much of the research focused on NOM adsorption to colloids and nanoparticles has focused on uncoated inorganic particles. For coated NPs, it is important to understand the interactions between the initial "engineered" coatings and "natural" coatings that result from the adsorption of NOM in natural waters. In previous work we demonstrated, on the basis of electrophoresis measurements, that SRHA adsorbs to AuNPs stabilized by five different organic capping agents. [21] The results reported here support those findings. However, the exact nature

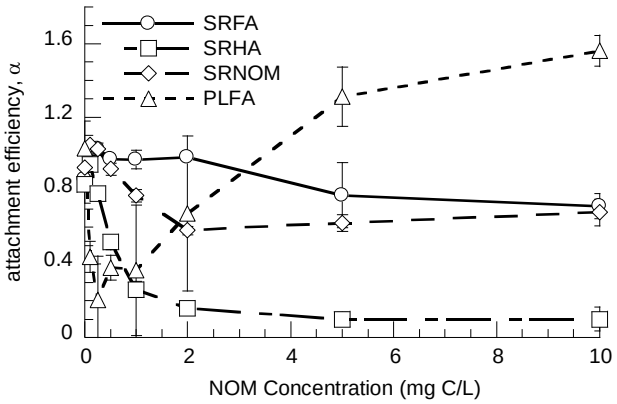

Fig. 4 The influence of NOM concentration of cit-AuNP colloidal stability. Attachment efficiencies as a function of DOC for 1 mg/L cit-AuNPs in 80 mM KCl and varying concentrations (0-10 mg C/L) of each of the four NOM isolates.

of the interactions between NOM and coated AuNPs remains unclear. Citrate molecules have been shown to form inner-sphere complexes with gold[36-38] and TiO_2[31] and likely exist on the surface as the fully deprotonated citrate anion.[39] When placed in contact with other capping agents, citrate can either be replaced[40] or overcoated[41] depending on the competing molecule. Additional work is necessary to determine which method described NOM adsorption to cit-AuNPs.

NOM concentration effects

Differences in aggregation behavior between the cit-AuNPs in
contact with the different NOM isolates carried over to the effects of NOM concentration. Fig. 4 details the influence of NOM concentation on the attachment efficiency of AuNPs in the presence of the four NOM isolates in 80 mM KCl. 80 mM was chosen for these trials because at this ionic strength cit-AuNPs are in the diffusion limited regime and (based on the CCC determinations shown in Fig. 3) the presence of NOM would likely provide a moderate degree of stabilization for all four NOM isolates. Raw TRDLS data for each of the four NOM isolates can be found in Figs. S5-S8†.

For cit-AuNPs in the presence of SRFA, it is clear from Fig. 4 that 2-5 mg C/L as SRFA is necessary to significantly influence the colloidal stability of cit-AuNPs. At 5 and 10 mg C/L as SRFA, initial growth rates were roughly 70% of the diffusion limited rates for cit-AuNPs in the absence of NOM. However, after an initial period of rapid increase in D_h, aggregation was much slower (Fig. S5†). In fact, after 5 minutes, aggregation was extremely slow in the presence of 10 mg C/L as SRFA. A D_h of approximately 54 nm was reached after 5 minutes for 10 mg C/L as SRFA, suggesting an adsorbed layer thickness of 21 nm. The behavior of cit-AuNPs in SRFA at 10 mg C/L was very similar to the behavior seen for 1 mg/L SRHA at higher ionic strengths (Fig. 2b). Based on the discussion above, this initial increase in D_h is attributed to increased NOM adsorption rather than NP-NP aggregation.

In contrast to the SRFA results, concentrations of SRHA as low as 0.25 mg C/L increased the stability of the cit-AuNPs in 80 mM KCl. Profiles of D_h vs. t were indicative of SRHA adsorption and subsequent stabilization at concentrations of 0.5 mg C/L and above (Fig. S6†). The influence of SRHA plateaus at approximately 1 mg C/L, suggesting that the adsorption capacity reached a maximum. Unfortunately, it was not possible to corroborate this using standard isotherm techniques due to the limited quantity and relatively high cost of the AuNPs. At concentrations $\geq$ 1 mg C/L as SRHA there were minimal changes in D_h upon addition of 0.8 mM KCl. Also, the D_h in the presence of 0.5 mg C/L was larger that that at higher NOM concentration, suggesting that perhaps there is some NP aggregation during the initial few minutes when the SRHA is adsorbing to the particles, albeit with a decreased driving force at the lower NOM concentration. This behavior disappears at SRHA concentrations greater than 1 mg C/L, perhaps due to increased adsorption kinetics. The fact that adsorbed layer thicknesses are small is in line with the hypothesis that at low ionic strengths, molecules assume a flat conformation on the NP surface.[9]

The observed differences in the concentration effects for SRFA and SRHA suggest that either SRHA has a

higher adsorption capacity on the cit-AuNP surfaces, or that for the adsorption of a fixed amount of NOM, SRHA has a greater influence on NP stability than the same amount of adsorbed SRFA. Such behavior could be related to the differences in physico-chemical properties such as molecular weight or chemical functionality that affect adsorption, or conformation on the NP surface (*vide infra*)

The effect of SRNOM concentration on cit-AuNP agregation was essentially a hybrid between the effects of SRFA and SRHA. In comparison with SRFA, SRNOM began to stabilize NPs at a lower concentration (0.5 mg C/L), consistent with the SRHA results. However, the stabilizing effect appeared to level off at an elevated collision efficiency consistent with the results from the SRFA. At SRNOM concentrations of 5 and 10 mg C/L, AuNPs grew rapidly for the first 3-5 minutes, but were quite stable at D_h = 50-70 nm beyond that point, suggesting adsorbed layer thicknesses of 20-30 nm (Fig. S7†). These results are consistent with the fact that the SRNOM contains both SRHA and SRFA fractions. The fact that the humic fraction is a much smaller percentage of the total would explain both the increased stabilizing effects at lower NOM concentration, as well as the SRFA-like behavior with increasing NOM concentration.

Aggregation of cit-AuNPs in the presence varying concentrations of PLFA was substantially different than for AuNPs in the presence any of the other NOM isolates. Consistent with the CCC results, low concentrations of PLFA (0.1-2 mg C/L) effectively stabilized the cit-AuNPs. However, rapid aggregation occurred in the presence of >2 mg C/L as PLFA. Although the collision efficiency calculations suggest enhanced aggregation, inspection of the raw data (supplementary information) reveal slightly faster initial rates of change of D_h, some of which are likely due to the rapid adsorption/conformational changes described above. After appoximately 5 minutes, the particle sizes in the absence and presence of PLFA (5 and 10 mg C/L) were quite similar (Fig. S8†).

The results at low NOM concentrations are consistent with the results as a function of ionic strength, where PLFA was more effective at stabilizing the cit-AuNPs than SRFA or SRNOM. The rapid destabilization of particles in the presence of higher concentrations of PLFA could be explained by bridging flocculation induced by favorable interactions between PLFA molecules on adjacent AuNPs that arise at higher surface coverages or when free PLFA molecules remain in solution.[6] As discussed in the introduction, this type of behavior has commonly been seen in solutions containing divalent cations. In this case, with monovalent electrolytes, the behavior could be explained by favorable hydrophobic interactions between PLFA coated particles that occur at increased surface coverages (*vide infra*). Continued efforts are underway to understand the underlying mechanisms.

Correlating AuNP stability with NOM properties

Building on the work of Deonarine *et al*., who recently examined trends in the initial growth rates (combined precipitation and aggregation) of ZnS NPs with various NOM isolates[19], it was our initial hope to correlate CCCs for the four NOM isolates with the physico-chemical properties of the NOM. Because the CCC is theoretically independent of nanoparticle concentration[42] and implicitly incorporates the influence of ionic strength, we believed that it would be a more robust quantitative tool for relating the stabilizing effects of NOM with physico-chemical properties. For example, such relationships have been used to develop structure-property relationships describing the colloidal stability of functionalized carbon nanotubes.[43]

As is clear from the data presented in Fig. 2, it is highly likely that NOM adsorption is also influencing the initial rates of change in D_h. This fact combined with the substantial amount of overlap in the attachment efficiency data in the region of the CCC for the four NOM isolates, the somewhat subjective nature of choosing which data to use to define the diffusion limited regime for purposes of calculating the CCC, and the limited number of NOM isolates resulted in this effort not being fruitful.

Because the NOM isolates investigated in this work are a subset of those used by Deonarine *et al.* we can evaluate the differences in NP stability in the context of that work. For ZnS nanoparticles, the different stabilizing effects of 9 different humic and fulvic acids were attributed primarily to properties related to steric effects; ZnS NPs in the presence of humic substances with higher molecular weight and higher $SUVA_{280}$ consistently had slower growth rates. In a similar analysis, we compared the attachment efficiencies of cit-AuNPs in the presence of 1 mg C/L of each of the NOM isolates in 80 mM KCl (Fig. 4). Under these conditions, stabilizing effects of the four NOM isolates were as follows SRHA > PLFA > SRNOM > SRFA. In general, these trends were evident at other NOM concentrations as well.

SRHA has the highest molecular weight and also the highest aromatic carbon and $SUVA_{280}$ values[19], consistent with the previous work. The fact that SRNOM provide stability intermediate between SRHA and SRFA, but closer to that of SRFA is reasonable based on the fact that SRNOM contains primarily SRFA with a smaller amount of

SRHA. However, PLFA, a relatively small fulvic acid with very low aromatic content, provides a substantial amount of stability. Furthermore, PLFA appears to have a greater adsorption density than SRFA at the same ionic strength, and also exhibits a strong destabilizing effect at higher NOM concentrations. PLFA has a much higher alophatic carbon content as well as a higher C:O molar ratio,[19] suggesting that hydrophobic interactions may play an important role in PLFA adsorption and inter-particle interactions.

In general, larger molecular weight NOM isolates appear to provide greater stability and resist destabilization by compression of the electral double layer to a greater extent. However, electrostatic interactions are still important as evidenced by the influence of ionic strength. Clearly the extent of NOM adsorption, the conformation on the NP surface, and the interactions between NOM molecules on adjacent particles are important factors influencing the initial growth rates measured in this work. Efforts are necessary to decouple the NOM adsorption and NP-NP aggregation processes in order to better understand the influence of NOM physico-chemical properties on NP stability.

Summary and Conclusions

As predicted based on the large body of research focused on the stabilizing effect of NOM on natural colloidal stability, it has been shown that four different NOM isolates act to stabilize cit-AuNPs with respect to aggregation. The resulting stability appears to be due to adsorption of the NOM onto the surfaces of the particles although questions remain regarding the nature and mechanisms of these processes. The adsorption process appears to occur over the course of 3-5 minutes upon an increase in ionic strength and is accompanied by NP aggregation in some instances. For the larger molecular weight SRHA at all concentrations and higher concentrations (> 5 mg/L) of lower molecular weight fractions (SRFA and PLFA), it appears that increased NOM adsorption at moderate ionic strengths results in significant increases in the hydrodynamic diameter of the particles, resulting in adsorbed layer thicknesses ranging from 4-30 nm. Preliminary SAXS analysis supports the conjecture that this change in size is not due to NP-NP aggregation. Although the adsorbed NOM layer likely imparts some steric stabilization, ionic strength effects are still evident in the aggregation behavior of NOM-coated AuNPs, suggesting that electrostatic effects remain important.

Despite similarities in the general aggregation trends between the four NOM isolates, each behaved differently in terms of the ionic strength and NOM concentration that resulted in stable NP suspensions. Low concentrations of SRHA and PLFA (≈0.25 mg C/L) were required to induce AuNP stabilization while higher concentrations of SRFA (> 2 mg/L) were required at the same ionic strength. Furthermore, SRNOM, which is largely a mixture of SRHA and SRFA displayed characteristics intermediate between these two fractions with respect to Au-NP stability. At elevated concentrations of PLFA, AuNPs were destabilized, possibly by bridging flocculation induced by favorable hydrophobic interactions between adsorbed PLFA molecules on adjacent NPs.

Clearly, both the type and concentration of NOM, along with the ionic strength of the system are important factors in determining the colloidal stability. Relatively few studies have focused on the influence of NOM type and concentration. We feel these results are a promising first step towards better understanding, and ultimately predicting, NOM-NP interactions and the resulting effects on NP fate and transport. However, much remains to be done to achieve this goal. Ongoing work is focused on extending these findings to other NOM isolates, other AuNPs with different capping agents and core materials, and incorporating the effects of divalent electrolytes and waters with ionic character simlar to relevant natural waters. Also, we are currently attempting to quantify and characterize NOM adsorption and the nature of the NOM-NP interactions through the use of advanced surface analytical techniques.

Acknowledgements

We thank Howard Fairbrother at Johns Hopkins University for his insightful comments and advice, Sarah Williams and Dylan Stankus at Oregon State University for their contributions to the early portion of this work and Erik Richman at the University of Oregon for assistance with the SAXS analysis. This work was funded by the Air Force Research Laboratory (agreement number FA8650-05-1-5041) and the National Science Foundation (Award 1067794).

Notes

[a] *School of Chemical, Biological and Environmental Engineering, Oregon State University, 103 Gleeson Hall, Corvallis, OR, 97331, USA. Fax: +1 541-737-4600; Tel: +1 541-737-9911; E-mail: jeff.nason@oregonstate.edu*
[b] *School for Engineering of Matter, Transport and Energy, Arizona State University, 501 E. Tyler Mall, Tempe, AZ, USA. E-mail: twcallah@asu.edu*
† Electronic Supplementary Information (ESI) available: Figs. S1-S4 contain SAXS data for cit-AuNPs in the presence and absence of SRHA and Figs. S5-S8 contain TR-DLS data for cit-AuNPs in various concentrations of the 4 NOM isolates. See DOI: 10.1039/b000000x/
‡ *E-mail: mcdowels@onid.orst.edu*

References

1 Woodrow Wilson International Center for Scholars, *The Project on Emerging Nanotechnologies: Nanotechnology Consumer Product Inventory*, http://www.nanotechproject.org/inventories/consumer, Accessed December, 2011, 2011.
2 M. R. Wiesner, G. V. Lowry, P. Alvarez, D. Dionysiou and P. Biswas, *Environmental Science & Technology*, 2006, **40**, 4336-4345.
3 M. R. Wiesner, G. V. Lowry, K. L. Jones, J. M. F. Hochella, R. T. Di Giulio, E. Casman and E. S. Bernhardt, *Environmental Science & Technology*, 2009, **43**, 6458-6462.
4 J. Buffle, K. J. Wilkinson, S. Stoll, M. Filella and J. W. Zhang, *Environmental Science & Technology*, 1998, **32**, 2887-2899.
5 C. L. Tiller and C. R. Omelia, *Colloids and Surfaces a-Physicochemical and Engineering Aspects*, 1993, **73**, 89-102.
6 E. Tipping and D. C. Higgins, *Colloids and Surfaces*, 1982, **5**, 85-92.
7 K. L. Chen and M. Elimelech, *Journal of Colloid and Interface Science*, 2007, **309**, 126-134.
8 R. F. Domingos, N. Tufenkji and K. J. Wilkinson, *Environmental Science & Technology*, 2009, **43**, 1282-1286.
9 A. Franchi and C. O'Melia, *Environmental Science & Technology*, 2003, **37**, 1122-1129.
10 H. Hyung, J. D. Fortner, J. B. Hughes and J.-H. Kim, *Environmental Science & Technology*, 2007, **41**, 179-184.
11 A. A. Keller, H. T. Wang, D. X. Zhou, H. S. Lenihan, G. Cherr, B. J. Cardinale, R. Miller and Z. X. Ji, *Environmental Science & Technology*, 2010, **44**, 1962-1967.
12 Y. Zhang, Y. S. Chen, P. Westerhoff and J. Crittenden, *Water Res*, 2009, **43**, 4249-4257.
13 Y. Zhang, Y. S. Chen, P. Westerhoff, K. Hristovski and J. C. Crittenden, *Water Res*, 2008, **42**, 2204-2212.
14 S. W. Bian, I. A. Mudunkotuwa, T. Rupasinghe and V. H. Grassian, *Langmuir*, 2011, **27**, 6059-6068.
15 A. R. Petosa, D. P. Jaisi, I. R. Quevedo, M. Elimelech and N. Tufenkji, *Environmental Science & Technology*, 2010, **44**, 6532-6549.
16 D. Grasso, K. Subramaniam, M. Butkus, K. Strevett and J. Bergendahl, *Re/Views in Environmental Science and Bio/Technology*, 2002, **1**, 17-38.
17 T. Phenrat, J. E. Song, C. M. Cisneros, D. P. Schoenfelder, R. D. Tilton and G. V. Lowry, *Environmental Science & Technology*, 2010, **44**, 4531-4538.
18 K. Yang, D. Lin and B. Xing, *Langmuir*, 2009, **25**, 3571-3576.
19 A. Deonarine, B. L. T. Lau, G. R. Aiken, J. N. Ryan and H. Hsu-Kim, *Environmental Science & Technology*, 2011, **45**, 3217-3223.
20 K. J. Wilkinson, J.-C. Negre and J. Buffle, *Journal of Contaminant Hydrology*, 1997, **26**, 229-243.
21 D. P. Stankus, S. E. Lohse, J. E. Hutchison and J. A. Nason, *Environmental Science & Technology*, 2011, **45**, 3238-3244.
22 J. Gao, S. Youn, A. Hovsepyan, V. L. Llaneza, Y. Wang, G. Bitton and J. C. J. Bonzongo, *Environmental Science & Technology*, 2009, **43**, 3322-3328.
23 R. D. Holbrook, C. N. Kline and J. J. Filliben, *Environmental Science & Technology*, 2010, **44**, 1386-1391.
24 S. Biggs, P. Mulvaney, C. F. Zukoski and F. Grieser, *Journal of the American Chemical Society*, 1994, **116**, 9150-9157.
25 M. Stobiecka, K. Coopersmith and M. Hepel, *Journal of Colloid and Interface Science*, 2010, **350**, 168-177.
26 K. L. Chen and M. Elimelech, *Langmuir*, 2006, **22**, 10994-11001.
27 K. L. Chen, S. E. Mylon and M. Elimelech, *Environmental Science & Technology*, 2006, **40**, 1516-1523.
28 K. L. Chen, S. E. Mylon and M. Elimelech, *Langmuir*, 2007, **23**, 5920-5928.
29 R. J. Hunter, ed., *Foundations of Colloid Science*, Second edn., Oxford University Press, Inc., New York, NY, 2001.
30 J. Ilavsky and P. R. Jemian, *Journal of Applied Crystallography*, 2009, **42**, 347-353.
31 I. A. Mudunkotuwa and V. H. Grassian, *Journal of the American Chemical Society*, 2010, **132**, 14986-14994.

32 K. L. Chen, B. A. Smith, W. P. Ball and D. H. Fairbrother, *Environmental Chemistry*, 2010, **7**, 10-27.

33 R. L. Malcolm, G. R. Aiken, E. C. Bowles and J. D. Malcolm, in *Humic Substances in the Suwannee River, GA: Interaction, Properties, and Proposed Structures*, eds. R. C. Averett, J. A. Leenheer, D. M. McKnight and K. A. Thorn, USGS, Denver, CO, Editon edn., 1989, vol. Open File Report 87-557, pp. 13-19.

34 A. W. P. Vermeer, W. H. van Riemsdijk and L. K. Koopal, *Langmuir*, 1998, **14**, 2810-2819.

35 L. C. McKenzie, P. M. Haben, S. D. Kevan and J. E. Hutchison, *Journal of Physical Chemistry C*, 2010, **114**, 22055-22063.

36 S. Floate, M. Hosseini, M. R. Arshadi, D. Ritson, K. L. Young and R. J. Nichols, *Journal of Electroanalytical Chemistry*, 2003, **542**, 67-74.

37 Y. Lin, G. B. Pan, G. J. Su, X. H. Fang, L. J. Wan and C. L. Bai, *Langmuir*, 2003, **19**, 10000-10003.

38 R. J. Nichols, I. Burgess, K. L. Young, V. Zamlynny and J. Lipkowski, *Journal of Electroanalytical Chemistry*, 2004, **563**, 33-39.

39 J. Kunze, I. Burgess, R. Nichols, C. Buess-Herman and J. Lipkowski, *Journal of Electroanalytical Chemistry*, 2007, **599**, 147-159.

40 T. Zhu, K. Vasilev, M. Kreiter, S. Mittler and W. Knoll, *Langmuir*, 2003, **19**, 9518-9525.

41 S. H. Brewer, W. R. Glomm, M. C. Johnson, M. K. Knag and S. Franzen, *Langmuir*, 2005, **21**, 9303-9307.

42 H. Holthoff, S. U. Egelhaaf, M. Borkovec, P. Schurtenberger and H. Sticher, *Langmuir*, 1996, **12**, 5541-5549.

43 B. Smith, K. Wepasnick, K. E. Schrote, H. H. Cho, W. P. Ball and D. H. Fairbrother, *Langmuir*, 2009, **25**, 9767-9776.